AMERICAN UNIVERSITY OF BEIRUT

COMPRESSIVE BEHAVIOR OF CONCRETE COLUMNS WRAPPED WITH HEMP FIBER REINFORCED POLYMER – AN EXPERIMENTAL STUDY

by
LEA JOSEPH GHALIEH

A thesis
submitted in partial fulfillment of the requirements
for the degree of Master of Engineering
to the Department of Civil Engineering
of the Faculty of Engineering and Architecture
at the American University of Beirut

Beirut, Lebanon
January 2017

AMERICAN UNIVERSITY OF BEIRUT

COMPRESSIVE BEHAVIOR OF CONCRETE COLUMNS
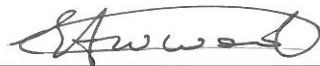WRAPPED WITH HEMP FIBER REINFORCED
POLYMER – AN EXPERIMENTAL STUDY

by
LEA JOSEPH GHALIEH

Approved by:

_____   _____
Dr. George Saad, Assistant Professor   Advisor
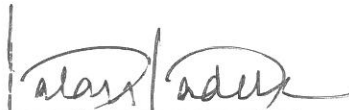Department of Civil and Environmental Engineering

_____   _____
Dr. Elie Awwad, Associate Professor   Co-Advisor
Lebanese University

_____   _____
Dr. Mounir Mabsout, Chairperson   Member of Committee
Department of Civil and Environmental Engineering

_____   _____
Dr. Salah Sadek, Professor   Member of Committee
Department of Civil and Environmental Engineering

January 31, 2017

AMERICAN UNIVERSITY OF BEIRUT

THESIS, DISSERTATION, PROJECT RELEASE FORM

Student Name: _____
Last   First   Middle

◯ Master's Thesis   ◯ Master's Project   ◯   Doctoral
Dissertation

☐   I authorize the American University of Beirut to: (a) reproduce hard or electronic copies of my thesis, dissertation, or project; (b) include such copies in the archives and digital repositories of the University; and (c) make freely available such copies to third parties for research or educational purposes.

☐   I authorize the American University of Beirut, to: (a) reproduce hard or electronic copies of it; (b) include such copies in the archives and digital repositories of the University; and (c) make freely available such copies to third parties for research or educational purposes
after: **One ----   year from the date of submission of my thesis, dissertation, or project.**
          Two ----   years from the date of submission of my thesis, dissertation, or project.
          Three ---- years from the date of submission of my thesis, dissertation, or project.

_____

Signature   Date

AN ABSTRACT OF THE THESIS OF

Lea Joseph Ghalieh   for   Master of Engineering
                                    Major: Civil Engineering

Title: Compressive Behavior of Concrete Columns Wrapped with Hemp Fiber Reinforced
 Polymer – an Experimental Study

Concrete confinement with fiber reinforced polymers is a method widely used for strengthening and rehabilitation purposes. The replacement of synthetic fibers used as external confinement (carbon, glass, and aramid) with natural fibers is a step to achieve a sustainable construction. In this research, an experimental study reports the efficacy of the use hemp fibers reinforced polymers as external confinement for concrete columns.

This study, aimed at understanding the effect of different parameters that may affect the structural behavior of concrete columns confined with fiber reinforced polymers. The test variables are: the number of the confining layers, the columns slenderness ratio, the addition of transverse steel reinforcement. Uniaxial compression test was done for a total number of 36 specimens, 30 of which are made of plain concrete and 6 with added transverse reinforcement.

The axial stress-strain curves, structural ductility measured by fracture energy and failure modes were analyzed. Also, the applicability of existing stress and strain models available in the literature is checked. It was found that the number of confining layers has a significant effect on the confinement effectiveness and ductility. Small numbers of confining layers lead to insufficient confinement. The column slenderness ratio also significantly affects the axial compressive strength and ductility of the confined samples. As the slenderness ratio increases, the confinement effectiveness and ductility decrease. The conjunction of transverse steel reinforcement with external confinement lead to a better confinement effectiveness. This study gave promising results vis-à-vis the use of natural fibers as external confinement despite the tensile strength of hemp FRP that are significantly lower than that of synthetic FRP.

CONTENTS

ILLUSTRATIONS

TABLES

CHAPTER 1

INTRODUCTION

The confinement of different structural elements such as columns, beams and walls is a method widely used for either strengthening or rehabilitation purposes of concrete structures. Many existing structures worldwide are either in need of rehabilitation due to deterioration from corrosion, poor detailing, earthquake load or strengthening due to increase in service load and others.

1.1. Thesis significance

The technique of concrete confinement with fiber reinforced polymers (FRP) has progressed over the last years at a rapid rate. Experimental studies proved that providing external confinement to concrete cylinders with fiber reinforced polymers substantially enhanced both the axial compressive strength and the ductility of the concrete specimen. Concrete jacketing started with the use of synthetic material, mainly carbon and glass polymers, as external confinement. These synthetic fibers reinforced polymers have high mechanical and physical properties that are attractive for structural applications.

On the other hand, with the increase of environmental concerns, the use of natural, bio-based fibers as a replacement of synthetic polymers is gaining popularity nowadays. Some natural fibers such as hemp, banana, coir, jute, flax, sisal and many more have the potential to replace the synthetic materials as they also have attractive physical and mechanical properties.

These natural fibers can be used not only as external confinement of structural element but also in the cementitious matrices.

The use of natural fibers as a concrete confinement has several environmental advantages in comparison with the synthetic fibers. First, among these environmental advantages is renewability, the natural fibers are renewable material and hence can replenish with ecological cycles and annual crops. They can be readily available almost anywhere in the world and do not need substantial non-renewable fossil resources in their production. One other advantage is carbon neutrality; the natural fibers have zero carbon footprints. Therefore, the difference between the carbon dioxide absorbed during the growth of the natural fibers and the carbon dioxide released in the atmosphere during the production, processing, use, and disposal of these fibers is zero. Also, the natural fibers yield agricultural residues that can be used in different applications and can be composted and used to improve the soil structure. Furthermore, the environment is facing a serious problem of accumulation of polyethylene (PE) that is non-degradable in soils; therefore, another advantage of the natural fibers is biodegradability. As a result, the use of natural fibers will have less harmful impact on the environment as compared to the use of other synthetic fibers and will contribute towards having sustainable development. (Sen & Reddy, 2014)

1.2. Thesis objective

The purpose of this study is to investigate the efficacy of the use of natural hemp fibers as external confinement for plain concrete columns. Concrete confinement is a method widely used for strengthening and rehabilitation purposes. Concrete confinement increases both the ultimate strength and ductility of structural members. This method has started with the use of synthetic fibers (carbon, glass and aramid) as external confinement. Nowadays, with the increase of the environmental concerns and with the aim to achieve a sustainable construction, the replacement of the synthetic fibers by natural fibers has recently started to be investigated.

The structural behavior of concrete columns confined with fiber reinforced polymers is affected by various parameters. These parameters include the type of the fiber used as a confining layer, the number of the confining layers, the column slenderness ratio, the shape of the column cross section, the cross-sectional area, the strength of the concrete and the addition of longitudinal and transverse steel reinforcement.

The investigated parameters in this study are limited to the number of the confining layer, the column slenderness ratio, and the addition of transverse spiral steel reinforcement.

The effect of the thickness of the confining layers will be checked by providing different number of confining layers of hemp fiber reinforced polymers. The number of layers checked are: 1, 2 and 4 layers with an overlap equal to half the perimeter of the cylinder for all cases. The column slenderness ratios will vary from 1.5 up to 3 with an interval of 0.5. The addition of steel reinforcement will be limited to the addition of transverse spiral steel reinforcement.

CHAPTER 2

BACKGROUND AND LITERATURE REVIEW

The literature review is done to assess two key items necessary for this study. The first part is to gather available information from existing studies regarding retrofitting techniques for existing columns using synthetic fibers, mainly the columns confinement technique. The second is to review the available studies on the natural fibers and their application as retrofitting material. The results of the search showed abundant information about retrofitting techniques using synthetic fibers. On the other hand, the use of natural fibers as a retrofitting material is deemed to be a new technique and therefore extensive testing is required.

2.1. Retrofitting techniques

The performance of any structural member is affected by several factors. These factors may include the deterioration of these structures due to the actual use and aging, the exposure of the existing structures to extreme natural and environmental events such as earthquakes and floods, and errors in the design and construction.

For example, in the case of road infrastructure, the transport of heavier payloads is now possible with the advances in transportation logistics, also the new highway management systems have led to increase in traffic volumes. These increases will therefore translate into higher demand loads for bridges that may outcome their rated capacities.

Also, some structures such as bridges and highways are exposed to repeated loadings. Even if these applied cyclic loads are less than the static capacity of the structure, they can cause a fatigue failure. (ACI Committee 215, 1975)

Moreover, it is possible that some of the existing structures are used for a different purpose than the one they were intended for. For example, an existing classroom may be later transformed into a library. These extra imposed loads may have not been taken into consideration in the original design of the facility.

Besides, structures constructed several decades do not meet the recent changes in seismic design codes.

Therefore, these factors stress the need to retrofit or strengthen existing structures in order to meet the codes requirements. Two different approaches exist when a building does not meet the code requirements. The first approach is to demolish the existing structure and replace it with a new one, the second approach is to retrofit the structure in order to increase its load-carrying capacity.

Kahn et al. favor the alternative of retrofitting the existing structure rather than demolishing and rebuilding it. The structure demolition is found inconvenient and usually not desirable mainly because of the high capital outlay needed for new constructions, also from the disturbances that come along with demolishing and rebuilding structures such as road closures and cleanups. The upgrading approach is therefore more viable since it minimizes the capital expenses while extending the useful life of the existing structure.(Kahn & Levinson, 2011)

There are few alternatives when it comes to upgrading existing structures. One alternative is pouring more concrete to the existing structural members to increase their

strength; however, this alternative is not desirable due to the significant increase of both the strengthened element dimensions and the imposed self-weight of the structure. Another alternative is providing steel plates to structural elements using construction-grade epoxies. The disadvantages of this upgrading technique is the addition of self-weight to the structure and the corrosion/rusting of the steel plates that deteriorates the bond between the plate and the structure. Also, this method is considered difficult to achieve for curved surfaces such as circular columns and irregular shapes.(Raithby, 1980)

A different strengthening technique is the bonding of fiber reinforced polymers on structural elements. This technique is gaining popularity nowadays for it is fast and efficient. Providing external confinement to structural element enhances both the ultimate strength and ductility of the member without a considerable addition of self-weight to the structure.(Gheorghiu et al., 2004)

2.2. Hemp Fibers

2.2.1. Origin and Properties of Hemp Fibers

Various natural fibers such as hemp, coir, flax, jute and many more have attractive mechanical properties for structural use. Hemp fiber also known as *Cannabis Sativa L.* is an annual crop that has been grown for approximately 12,000 years. This crop is mainly found nowadays in the European Union, Central Asia, Philippines and China(Shahzad, 2011). Hemp fiber was mainly used in the textile, clothing, ropes and canvas industries. Nowadays, they are used in non-textile applications. Hemp fibers are now used in building materials, insulation, paper and pulp, and as bio-composites for automobile industries.

6

Many factors may influence the physical and mechanical properties of hemp fibers. Some of these factors are: geographic origins, age, diameter of the fiber, amount of rainfall during growth etc. The variability in the physical and mechanical properties of hemp fibers constitute their major drawback. (Khan, 2011)

Figure 1. Hemp Plant.

Placet has performed different experiments on hemp fibers. In his study, hemp fibers were subjected to a harmonic stress, and on the contrary to all expectations the application of this periodic stress did not lead to any fatigue in the material, but on the contrary it increased the fiber rigidity by a factor of 1.6, the Young's modulus of elasticity by 1.67 and decreased in its damping capacity by a factor of 2. After several cycles, the latter mechanical properties tend to stabilize, validating the "adaptation" phenomenon.(Placet, 2009)

Some relevant mechanical properties of some natural fibers are determined by Placet are listed in table 1.

Table 1. Properties of natural fibers determined by Placet.

Property	E-glass	Flax	Hemp	Jute	Ramie	Coir	Sisal	Abaca	Cotton
Density	2.55	1.4	1.48	1.46	1.5	1.25	1.33	1.5	1.51
Tensile Strength $X 10E^6 N/m^2$	2400	800-1500	550-900	400-800	500	220	600-700	980	400
E- Modulus (Gpa)	73	60-80	70	10-30	44	6	38	-	12
Specific Modulus (E/Density)	29	26-46	47	7-21	29	5	29	-	8
Elongation at Failure (%)	3	1.2-1.6	1.6	1.8	2	15-25	2-3	-	41343
Moisture Absorption (%)	-	7	8	12	12-17	10	11	-	41511
Price/Kg ($), Raw (mat or Fabric)	1.3	1.5	0.6-1.8	0.35	1.5-2.5	0.25 - 0.5	0.6 -0.7	1.5-2.5	1.5-2.2

2.2.2. Hemp fiber treatment

Natural fibers such as hemp, coir, jute and banana contain hydroxyl groups (OH), these groups react with polymer matrices and hence create the bond in polymer composites. However, natural fibers are covered with waxy material that hinder the hydroxyl groups from reacting with polymer matrices. This may result in ineffective bond between the fibers and the matrices leading to debonding problems and voids in the composites.(Sawpan, 2011)

Chemical treatment is an effective tool used to remove the fiber impurities that affect the bond between the fibers and the polymer matrices. Sawpan et al. treated hemp fiber with:

- Alkali treatment: A solution of 5% by wt. sodium hydroxide

- Silane treatment: A solution of 0.5% by wt. silane coupling agent prepared in acetone

- Maleic anhydride treatment: A solution of 0.5% by wt. maleic anhydride

Only the alkaline treatment increased the average tensile strength of fibers compared to untreated fibers. The increase is a result of increased cellulose crystallinity and therefore the exposure of OH groups.

2.3. Concrete confinement

2.3.1. Action of FRP confinement

FRP confining layers provide lateral confinement to a concrete structural member. The structural member expands laterally when subjected to an axial compressive force. The expansion that the structure undergoes is confined. Hence, the FRP jacket is loaded in tension and in the hoop direction.

The confining pressure increases with the increase of lateral strain and this is due to the brittle behavior of FRP material. Unlike steel, FRP is brittle by nature and does not yield. The action of FRP confinement is illustrated in figure 2.
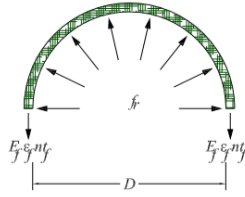
Figure 2. Action of FRP confinement.

E_f: tensile modulus of elasticity of FRP

n: number of plies of FRP reinforcement

t_f: nominal thickness of one ply of FRP reinforcement

ε_{fe}: effective strain level in FRP reinforcement attained at failure

D: diameter of compression member of circular cross section

The maximum confining pressure f_l due to FRP jacket is therefore calculated using the following equation:

$$f_l = \frac{2E_f n t_f \varepsilon_{fe}}{D}$$

2.3.2. Stress-strain Curves type

The vast majority of FRP confined concrete exhibits an ascending bi-linear shape with a transition zone around the maximum strength of unconfined concrete. In this type of stress-strain curve, the ultimate stresses and strains are reached simultaneously, and a significant enhancement in both the ultimate strength and ductility is noticed. Figure 3(a) illustrates the ascending type of stress-strain curve.

However, in some existing tests, the stress-strain curves show a post-peak descending part. In this case the maximum compressive strength is reached before the rupture of the FRP jacket. The stress-strain curve in this case may end at a stress value (the stress value corresponding to the ultimate stain) smaller or larger than the compressive strength of unconfined concrete.

This difference in behavior of confined concrete is mainly due to the FRP mechanical properties.(Aire et al., 2001; Harries & Kharel, 2002; Xiao & Wu, 2003).
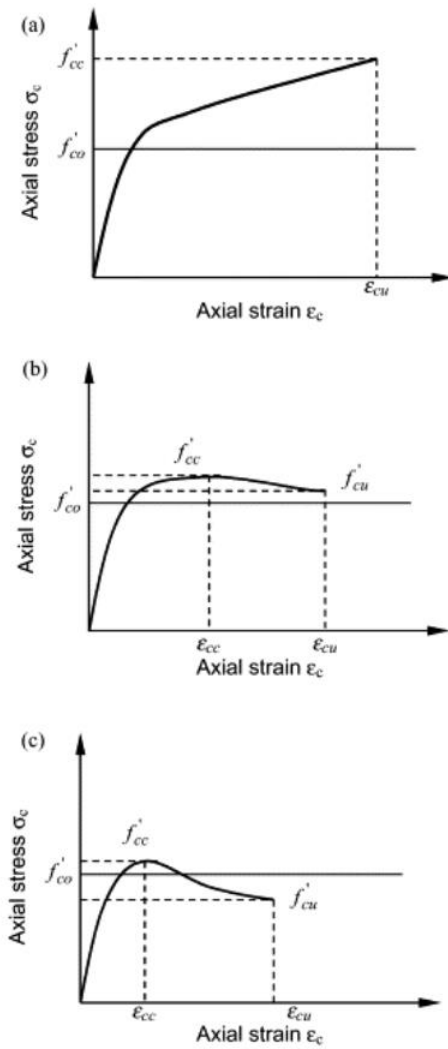
Figure 3. Classification of stress–strain curves of FRP-confined concrete. (a) Increasing type; (b) Decreasing type with f'$_{cu}$ ≥ f'$_{co}$; (c) Decreasing type with f'$_{cu}$ < f'$_{co}$. (Lam & Teng, 2003)

Therefore, the decreasing type of stress-strain curves can be divided into two parts depending on the concrete stress f'_{cu} corresponding to the ultimate strain. According to Lam and Teng, if the value of f'_{cu}, the stress at which the stress strain curve terminates, is smaller than the maximum compressive strength of unconfined concrete f'_{co} as illustrated in figure 3(c) the specimen is considered to be insufficiently confined and there is no

considerable enhancement in the compressive strength of the confined specimens. Such

cases of insufficient confinement should not be allowed in design. However, if the value of

f'_{cu} is larger than the maximum compressive strength of unconfined concrete f'_{co} as

illustrated in figure 3(b) the specimen is considered as sufficiently confined.

Lam and Teng used a database consisting of 76 specimens confined with carbon,

glass or aramid FRP existing in the literature. Based on their analysis oriented model, if the

confinement ratio $\dfrac{f_l}{f'_{co}}$ is larger than 0.07 an ascending post-peak branch is expected leading

to a considerable strength enhancement. For the case of confined specimens with a

confinement ratio less than 0.07 a stress-strain curve with a descending post-peak branch is

expected and no considerable strength enhancement is assumed. On the other hand,

Mirmiran et al. used a more conservative confinement ratio criterion of 0.15. However,

these criterions are based on the results of concrete confined with synthetic fibers. The

applicability of these criterions is questionable with the use of natural fibers that have lower

mechanical properties than the synthetic fibers(Lam & Teng, 2003; Mirmiran et al., 1998;

Spoelstra & Monti, 1999).

2.4. Confinement using synthetic fibers

A review of the literature showed that it has abundant information about synthetic

fiber reinforced polymers used as external confinement for concrete columns. The synthetic

materials are mainly carbon, glass and aramid. Various structural elements confined with

fiber reinforced composite sheets were investigated.

In their research, Demers et al (1999) investigated different parameters that can affect the structural behavior of reinforced concrete columns in compression. The parameters studied in their research were: the compressive strength of concrete, the amount of longitudinal steel reinforcement, the amount of transverse steel reinforcement, the corrosion of steel reinforcement and the damage of concrete. The two levels of the compressive strength f_c' that were used in the study were 25 and 40 MPa. The amount of steel reinforcement in terms of longitudinal steel reinforcement ratio was changed from 0.014 to 0.035. The spacing, s, of transverse steel was also varied from 300 mm that represents an under reinforced shear reinforcement level to 150 mm. The corrosion of steel was simulated by reducing the diameters of the longitudinal bars; the reduction was about 5 mm. The last parameter that was investigated was the damage of concrete. This parameter is directly related to the behavior of concrete structures that are in need of rehabilitation. To reach a damaged condition of concrete, unconfined specimens were loaded to a peak value. Once this value was attained and the cracks became visible, the specimens were unloaded. Demers et al. then concluded that the compressive strength of concrete and the amount of longitudinal steel reinforcement have a significant effect on the strength of confined reinforced columns and on the confinement effectiveness. The amount of transverse steel reinforcement did not affect the compressive behavior of the specimens; however, Demers et al. suggested to investigate the effectiveness of the confinement with more closely spaced stirrups than the spacing adopted in their study. The corrosion of steel had no effect on the strength of the confined concrete. Unlike the unconfined damaged specimens, confined damaged specimens were able to restore their strength characteristics and reach a

load carrying capacity similar to that of an undamaged confined specimen.(Demers &
Neale, 1999)

In their research Benzaid et al. concluded that the composite wrapping enhances
the structural performance of concrete columns for both plain and reinforced concrete. The
compressive strength and ductility increase with the increase with the number of
composites layers.(Benzaid & Mesbah, 2014)

Pan et al (2007) investigated the effect of the column slenderness ratio on the load
carrying capacity of reinforced concrete columns wrapped with carbon FRP. The
slenderness ratios ranged between 4.5 and 17.5. The axial compression results showed a
significant decrease in the strengthening effect of FRP with increase of the slenderness
ratio. (Pan et al., 2007)

Cln-1 L/b=4.5   Cln-2 L/b=8   Cln-3 L/b=10   Cln-4 L/b=12.5   Cln-5 L/h=14   Cln-6 L/b=17.5

Figure 4. Columns with different slenderness ratios, Placet et al.

The reduction of the performance of the taller samples is due to buckling
instability of slender columns that causes reduction in both strength and ductility.
Increasing the column height significantly affects the confinement pressure of the confining

layer and hence leads to considerable losses in strength and ductility. (El-Hacha & Abdelrahman, 2013)

In their research Elsanadedy et al. checked the effect of the specimen diameter size on the load carrying capacity and ductility while holding both the slenderness ratio L/D and the confinement ratio constant; thus, different number of confining layers are provided leading to equal confinement ratio. It was concluded that with the same confinement ratio (4t/D), where "t" is the thickness of the confining layer there are no significant differences in the compressive strength and ductility for cylinders having different sizes. (Elsanadedy et al., 2012)

On the other hand, Silva et al. (2006) also investigated the effect of the size of cylinders on compressive failure of concrete columns wrapped with glass fiber reinforced polymers. They concluded that increasing the diameter of the cylinders, while keeping both the slenderness ratio and the thickness of the outer confinement constant, leads to a significant reduction in the strength of the cylinders. If the confinement ratio is not increased with the increase of the section size the results show a decrease in strength of the cylinders.(Silva & Rodrigues, 2006).

Plain concrete is generally known for its brittle failure when subjected to compressive stress. Transverse reinforcement was therefore used to restrain the lateral expansion of concrete, enhance the ductility and delay the concrete failure. The increase of ductility and strength using steel spirals as confinement for concrete were prominent.

Early studies showed that the confinement effectiveness is dependent on many parameters: (1) the use of spirals or ties transverse reinforcement, (2) the spacing on the

transverse steel reinforcement, (3) the volume of the transverse steel reinforcement to the volume of the concrete core and many more.

The past investigations showed that the maximum strength and its corresponding axial strain of concrete confined with transverse reinforcement can be represented by the relationship that governs the behavior of a concrete sample confined by a hydrostatic fluid pressure.

$$f'_{cc} = f'_{co} + k_1 f_l$$

$$\varepsilon_{cc} = \varepsilon_{co}(1 + k_2 \frac{f_l}{f'_{co}})$$

Where k_1 and k_2 are coefficients that are dependent on the concrete mix and the lateral pressure of the confinement.

Mander. et al proposed a unified stress-strain approach applicable for both circular and rectangular shaped transverse reinforcement.(Mander et al., 1988)

Almost all codes and available strength models concentrate on the additional compressive strength due to FRP confinement but neglect the effect of the transverse steel reinforcement. However, in real life situations, the confined concrete columns are subjected to two confinement actions: the FRP external confinement and the transverse steel reinforcement internal confinement.

From here the need for a confinement model that considers the interaction of both FRP external confinement and transverse steel internal confinement. Figure 5 illustrates both the internal confining effect of transverse steel reinforcement on concrete core and the external confinement effect of FRP wraps.
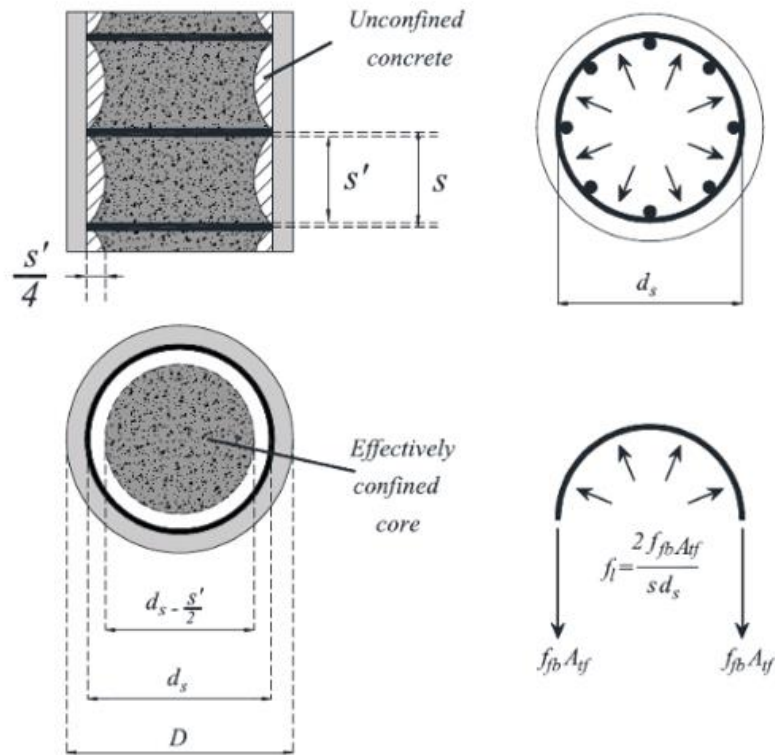
Figure 5. Effect of internal transverse steel reinforcement and external FRP confinement on concrete core.

Due to many environmental concerns, the effectiveness of the replacement of synthetic fibers by natural fibers has recently started to be investigated.

2.5. Confinement of concrete using natural fibers

Yan et al (2013) investigated the compression and flexural performance of flax fiber tube encased coir fiber reinforced concrete composite. The use of natural fibers as concrete confinement was accomplished by manufacturing natural fiber reinforced polymers tubes using the hand lay-up technique. Coir fiber is the reinforcement in the concrete (coir inclusion in the cementitious matrix) while the flax fiber (FFRP) tube

provides external confinement to the concrete cylinders. In their experimental research 36 specimens were tested; 18 short cylinders (inner diameter of 100 mm and length of 200 mm) tested under the uniaxial compression test and 18 long cylinders (inner diameter of 100 mm and length of 520 mm) tested under the third-point bending test. The test variables were FFRP tube thickness (number of layers, two and four layers used) and coir fiber inclusion percentage. In the axial compression test it was concluded that: concrete confinement leads to a considerable enhancement in compressive strength and ductility; a larger tube thickness leads to a better confinement effectiveness of the cylinder; and that coir fiber inclusion has no effect on the confinement effectiveness however it increases the axial strain and the ultimate compressive strength of the specimen. In flexure FFRP tube confinement enhanced the load carrying capacity and deflection of both plain concrete and coir reinforced concrete. (L. Yan & Chouw, 2013)

Sen et al. (2014) investigated the flexural behavior of sisal fabric reinforced polymer and compared it to the behavior of carbon and glass fabric reinforced polymer composite. Reinforced concrete beams were bonded externally with sisal fiber reinforced polymer (SFRP), carbon fiber reinforced polymer (CFRP), and glass fiber reinforced polymer (GFRP). The test variables were the nature of the fibers (sisal, carbon and glass) and the wrapping technique (no wrapping for control, full wrapping and strip wrapping i.e. only 50% of the total area was used for strengthening). The thickness of the confining material was determined in proportion to the tensile strength of each material used for wrapping. It was concluded that SFRC strengthening of RC beams showed increase in its flexural strength and improvement in the load deflection behavior and also exhibited the highest amount of ductility and delayed the formation of cracks. The sisal fibers failed

without rupture as in the case carbon FRP and without debonding as in the case of glass FRP. The highest load carrying capacity was for the fully wrapped beams, then the strip wrapped beams and the members with the least load carrying capacity were the control beam with no strengthening. The load carrying capacity of the natural sisal was comparable to that of the synthetic material.(Sena & Reddy, 2014)

In a different study, Yan et al. investigated the effect of the type of wrapping of concrete cylinders. Enhancement of the concrete axial compressive strength can be achieved by either FRP-wrapping of existing concrete columns (post-jacketing) or encasement of concrete in a hollow FRP tube for new construction (pre-jacketing).The difference between the two types of confinement consists in the bonding between the concrete and the flax polymer. FRP-wrapped concrete is adhesively bonded to the FRP; this adhesion is not needed in the case of pre-jacketing. Few studies are available on this subject in the literature. Mirmiran et al. stated that the FRP and concrete bond condition has no significant differences on the confinement effectiveness, while Deb and Bhattacharyya concluded that the bond influenced the ultimate strength of FRP-confined concrete remarkably. Therefore, the results of type of bond effect on FRP-confined concrete are conflicting. In their research, Yan et al investigated the effect of flax fiber reinforced polymer and concrete bond on the compressive behavior of flax fiber reinforced polymer–confined plain concrete and coir fiber reinforced concrete. Three types of bond were considered: concrete confined by flax fiber reinforced polymer tube (naturally bonded), flax fiber reinforced polymer tube with internal flax fiber reinforced polymer rings (mechanically bonded) and flax fiber reinforced polymer wrapping (adhesively bonded). The naturally bonded and mechanically bonded composites failed by the formation of a

single straight crack throughout the longitudinal direction of the tubes while in the case of

the adhesively bonded composite the crack initiated at one end of the jacket and then

propagated to the mid-length of the tube. Therefore, the type of FFRP and concrete bond

also affects the failure mode of the FFRP jacket. The confinement provided by the three

different FFRP systems enhanced the ultimate compressive strength and ultimate axial

strains of both PC and CFRC. Also, as shown in figure 3, all three types of bond enhanced

the ultimate strength of the confined concrete. However, the percentage of the confinement

effectiveness depends on the type of bond between the FRP material and concrete core. The

confinement effectiveness of FFRP tube, FFRP tube-ring and FFRP-wrapped-PC and

CFRC are 1.94, 1.69 and 1.65 and are 1.94, 1.73 and 1.62, respectively.(Deb &

Bhattacharyya, 2010; L. Yan et al., 2013)
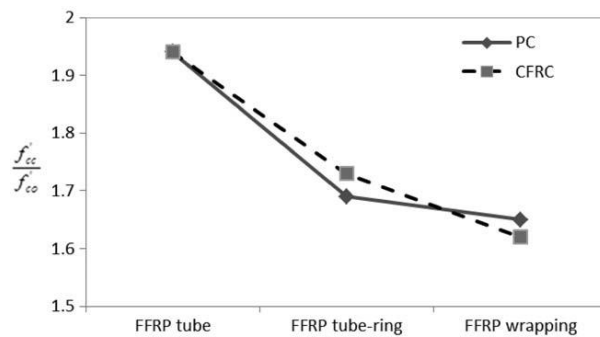
Figure 6. Confinement effectiveness based on the type of bond.

2.6. ACI Recommendations

ACI 440.2R-08 is the guide for the design and construction of externally bonded

FRP systems for strengthening concrete structures.

The maximum confined compressive strength f'$_{cc}$ is calculated as follow:

$$f'_{cc} = f'_c + \varphi_f 3.3 k_a f_l$$

Where:

f_c': unconfined cylinder compressive strength of concrete (MPa)

φ_f: reduction factor based on the committee judgment $\varphi_f = 0.95$

k_a: efficiency factor that accounts for geometry of the section. For circular columns $k_a = 1$

f_l: maximum confining pressure due to FRP jacket (MPa)

$$f_l = \frac{2E_f n t_f \varepsilon_{fe}}{D}$$

$$\varepsilon_{fe} = 0.55 \, \varepsilon_{fu}$$

E_f: tensile modulus of elasticity of FRP (MPa)

n: number of plies of FRP reinforcement

t_f: nominal thickness of one ply of FRP reinforcement (mm)

ε_{fu}: ultimate strain level in FRP reinforcement attained at failure (mm/mm)

ε_{fe}: effective strain level in FRP reinforcement attained at failure (mm/mm)

D: diameter of compression member of circular cross section, (mm)

A minimum value of 0.08 the ratio f_l / f_{co}' is recommended to ensure a sufficient confinement level.

The stress-strain model adopted by the ACI is the stress-strain model presented by Lam and Teng with the inclusion of a reduction factor based on the committee judgement. (Lam & Teng, 2003)
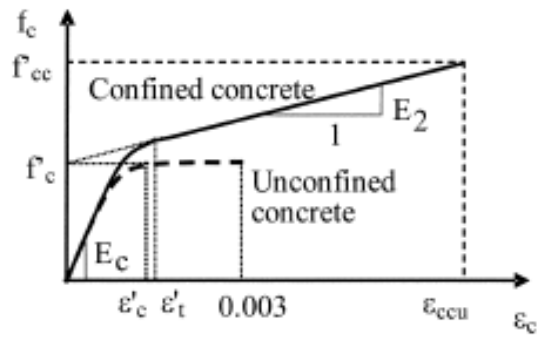
Figure 7. Lam and Teng's stress-strain model for FRP-confined concrete.

CHAPTER 3

EXPERIMENTAL PROGRAM

3.1. Introduction

In an attempt to gain a basic structural understanding of the behavior of confined plain concrete cylinders with FRP, some basic concepts had to be thoroughly studied; such as failure mechanisms for FRP confined columns, setup characteristics, and in particular, the efficacy of the use of hemp fibers as external confinement and their failure modes. Therefore, a preliminary study on small cylinders wrapped with hemp fibers had to be conducted.

This chapter is divided into two parts. The first part is a preliminary study on small plain concrete cylinders. The purpose of this part is to check the efficacy of the use of hemp fibers as external confinement. Twelve small cylinders, 10 cm diameter and 20 cm height, were cast; six samples were confined with hemp fibers. All the samples were tested in uniaxial compression and the results of the confined samples were compared to those of the unconfined sample. In the second part, the work done in the preliminary study is projected into a bigger scale project; the efficacy of use of hemp fiber is therefore checked on concrete columns. In this part different parameters that may affect the behavior and the efficacy of the use of hemp fibers as an external confinement were checked. The parameters checked in this study are the column slenderness ration (L/D), the number of

confining layers and the additional effect of transverse steel on the confinement effectiveness of fiber reinforced polymers.

The methodologies used in the study are thoroughly discussed in the next subsections.

3.2. Preliminary study

3.2.1 Hemp Fibers

3.2.1.1 Hemp Fibers Treatment

Based on the literature, natural fibers exhibit better results once their organic impurities are removed. In order to remove the impurities, hemp fibers have to be treated. The treatment adopted was the sodium hydroxide (NaOH) treatment used by Awwad et al.

In the preliminary study, raw hemp fibers were used, as shown in figure 5. The Hemp fibers were soaked in NaOH solution for 48 hours. The amount of NaOH dissolved in water was 6% by weight. After 48 hours, the fibers were washed with water abundantly and then the fibers were let to dry. (Awwad et al., 2012)

Figure 8. Hemp bundle.

3.2.1.2. Hemp Fibers Tensile test

      In order to fully understand the behavior of the hemp-confined cylinders. The tensile strength of the hemp fibers bundles was tested. The tensile testing was done using the ASTM D 3822-14 the 'Standard for Tensile Properties of Single Fibers'. Figure 6 shows a hemp fiber rope test setup. (StandardforTensilePropertiesofSingleFibers, 2014)
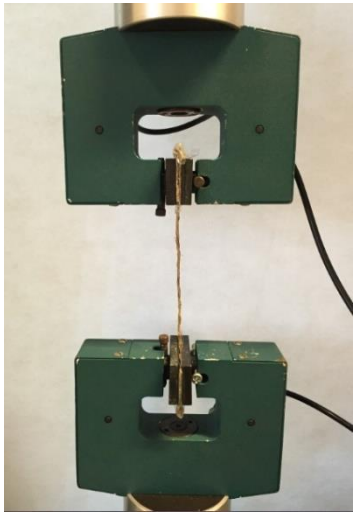
Figure 9. Tensile testing on hemp bundle.

The key testing points are listed below:

1- Gauge length: the selected gauge length, that is the clear distance between the two grips, is 100 mm. This gauge length was kept constant throughout the test.

2- Constant rate of extension: the rate of extension or pull was set 15 mm/min for all the fiber tests.

3- Clamps: clamps with flat jaws were used to grip the fiber specimens and minimize their slippage

26

The results showed a typical load-elongation curve. As the load increases, the fiber extension increases until it reaches a peak point at a certain point of extension. The load corresponding to the maximum point of extension is the maximum tensile load P_{max} that the fiber can carry. Because hemp fibers are brittle by nature, the fiber broke after reaching the maximum elongation.

Every fiber had a different load-elongation curve. Hence, the results showed a different tensile strength property. This variability in the results is due to the high variable nature of hemp fiber properties.

3.2.2. Concrete cylinders.

Twelve small cylinders were prepared (10cm diameter, 20 cm height), six of which were confined. The concrete mix consists of the following batching weights per cubic meter of concrete: 880 kg of small coarse aggregate, 810 kg of sand, 400 Kg of cement and 280 Kg of water (w/c = 0.7). Twelve specimens from the same batch were prepared. The experimental matrix is shown in table 2.

Four different groups of plain concrete cylinders were prepared:

- Control cylinders

- Epoxy coated cylinders: plain concrete cylinders coated only with epoxy were prepared, in order to check for the contribution of epoxy coating.

- Hemp fibers confined cylinders: plain concrete cylinders were wrapped with hemp fibers using epoxy.

27

- Hemp fibers confined grinded cylinders: cylinders were grinded in order to roughen the surface area and hence enhance the bond between the concrete and the hemp fibers.

Table 2. Experimental Matrix of the Preliminary Study.

Specimen Group	No. of specimens	No. of hemp layers	Diameter (mm)	Length (mm)
Control	3	-	100	200
Epoxy	3	-	100	200
Hemp	3	1	100	200
Grinded	3	1	100	200

Three fibers were twisted together manually to form one rope. The rope was prepared to have a designated length that can cover the perimeter of the concrete cylinder (100 mm diameter and 200 mm height) with an overlap of 157 mm (half perimeter) at both extremities of the cylinders. The rope was then wrapped around the cylinder using epoxy resin.

Figure 10. Unconfined and confined specimens.

Uniaxial compression test was then done on all the specimens with a constant rate of 0.2 MPa/s based on ASTM C39. The samples were axially compressed up to failure. Four linear variable displacement transducers (LVDTs) were aligned along the axial direction of the specimen in order to measure the axial strain. Readings from the four LVDTS were averaged and stress strain curves were plotted. (ASTM, 2010)

Figure 11. Preliminary study: Uniaxial compression test setup.

3.2.3 Preliminary results discussion

The stress strain curves of the concrete cylinders samples were averaged and plotted on the same graph. The curves are shown in figure 9.

In general, in the case of confined concrete cylinders, the samples display an approximate bi-linear behavior with a transition zone. The first ascending linear part of the stress strain curve is similar to the unconfined specimens; in this part the strain increases with the increase of the stress applied until it reaches a peak value. When the applied load exceeds the maximum strength that the cylinder can carry, the curve enters in a second linear region. In this region micro-cracks are developed in the concrete, the lateral expansion increases and hence the concrete confinement is fully activated to confine the concrete core. The concrete confinement leads to a considerable enhancement in the ductility and compressive strength of the concrete cylinder.
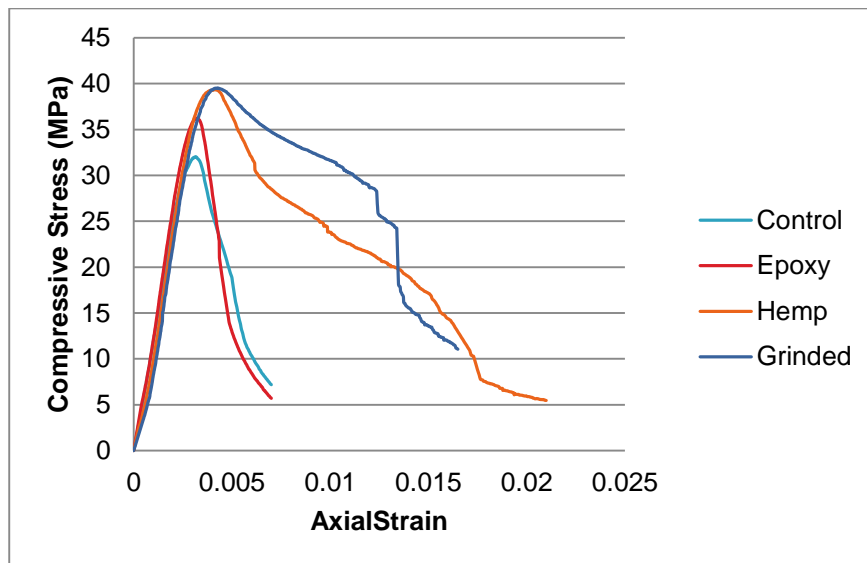
Figure 12. Stress-strain curves of preliminary study.

Table 3. Test results of preliminary specimens.

Specimen type	f'_{co} (MPa)	f'_{cc} (MPa)	ε_{co} (%)	ε_{cc} (%)	$\dfrac{f'_{cc}}{f'_{co}}$	$\dfrac{\varepsilon_{cc}}{\varepsilon_{co}}$
Control	32.03	-	0.316	-	-	-
Epoxy	36.23	-	0.322		-	-
Hemp	-	39.35	-	0.41	1.22	1.29
Grinded	-	39.51	-	0.427	1.23	1.35

Table 3 gives the results of specimens tested, where:

f'_{co}: the peak compressive strength of unconfined concrete.

f'_{cc}: the peak compressive strength of confined concrete.

$\dfrac{f'_{cc}}{f'_{co}}$: the confinement effectiveness.

ε_{co} is the axial strain for unconfined concrete at the corresponding peak compressive strength f'_{co}.

ε_{cc}: the axial strain for confined concrete at the corresponding peak compressive strength f'_{cc}.

$\dfrac{\varepsilon_{cc}}{\varepsilon_{co}}$: the axial strain ratio.

Providing external confinement to concrete cylinders gave promising results. The compressive strength is enhanced by approximately 22%. The ductility is also enhanced. For the case of hemp-confined cylinders the ductility is enhanced by 29%, whereas in the

case of grinded cylinders, where the concrete surface is roughened to increase the bond

between the hemp and the concrete surface, the ductility is enhanced by 35%.

Figures 13, 14, 15 and 16 display the failure modes of the control, epoxy, hemp

and grinded specimens respectively. The control samples are crushed and spalled and show

cracks that are more severe than the cracks present in the epoxy specimens. During the

compressive test, the confined specimens failed by a sudden rupture that generated a heavy

popping noise. A single fracture crack occurred, this crack is located approximately in the

middle of the concrete cylinder and is not straight due to the variability in the strength of

the hemp fibers. The concrete core of the confined specimens possessed large macro-

cracks. These macro-cracks indicate that the concrete core has failed before the confining

layer was ruptured. The confinement is activated due to the lateral expansion of the

concrete core once crushed.

Figure 13. Control specimens.

Figure 14. Epoxy coated specimens.

Figure 15. Hemp confined specimens.

Figure 16. Grinded hemp confined specimens

3.3. Concrete Columns

Based on the promising results found in the preliminary study, the effectiveness of the use of hemp fiber polymers as external confinement is checked for bigger scale columns. Three parameters that may affect the structural behavior of confined columns are checked. These parameters are the number of confining layers, the column slenderness ratio and the addition of spiral transverse steel reinforcement.

3.3.1. Experimental Program and Test Variables

3.3.1.1. Number of Confining Layers

In order to check the effect of the number of confining layers on the confinement effectiveness, the number of confining layers varied from 1, 2 and 4 layers and all other variables are held constant. An overlap equal to half the perimeter of the cylinder is provided for all the samples. The cylinders are made of plain concrete.

Table 4. Sensitivity on the number of confining layers.

Sensitivity on the number of confining layers			
Length (cm)	Diameter (cm)	Number of confining layers	Number of confined samples*
40	20	1	3
40	20	2	3
40	20	4	3
* samples wrapped with hemp fibers			9

3.3.1.2. Column Slenderness Ratio

The effect of the slenderness ratio will be checked by providing different lengths to the specimens while keeping the same diameter. The different slenderness ratios checked are: 1.5, 2, 2.5 and 3. The cylinders are made of plain concrete and are wrapped with two layers of hemp with an overlap equal to half the perimeter of the cylinder in all cases.

Table 5. Sensitivity on the slenderness ratio.

Sensitivity on L/D ratio					
Length (cm)	Diameter (cm)	L/D	Number of control samples	Number of confined samples*	Total
60	20	3	3	3	6
50	20	2.5	3	3	6
40	20	2	3	3	6
30	20	1.5	3	3	6
* samples wrapped with two layers of hemp fibers					24

3.3.1.2. Addition of Transverse Steel Reinforcement

This section only considers the confinement action of hemp FRP and spiral transverse reinforcement. Longitudinal reinforcement is not added to eliminate their confinement effect to concrete columns.

The effect of the addition of transverse reinforcement is checked by providing spiral stirrups. Transverse reinforcement was therefore used to restrain the lateral expansion of concrete, enhance the ductility and delay the concrete failure.

The transverse spiral steel reinforcement has a diameter of 6 mm. The concrete cover is 2.5 cm from all sides (top, bottom, right and left). The spiral consists of 7 hoops with a pitch "s" of 5 cm center to center.
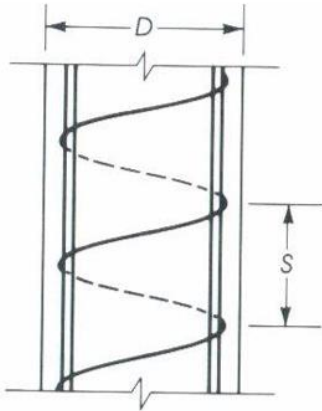
Figure 17. Schematic representation of concrete cylinders with spiral transverse reinforcement.

The cylinders are made of plain concrete with the addition of stirrups and are wrapped with two layers of hemp with an overlap equal to half the perimeter of the cylinder in all cases. The slenderness ratio is also held constant.

Table 6. Sensitivity on the addition of transverse reinforcement.

Sensitivity on addition of stirrups				
Length (cm)	Diameter (cm)	Number of control samples	Number of confined samples*	Total
40	20	3	3	6

3.3.1.3. <u>Test Matrix</u>

Table 7. Test Matrix.

Specimen Group	No. of Specimen	No. of Fabric Layers	Core Diameter D (mm)	Length (mm)	Transverse Steel
PC-30	3	-	200	300	NO
PC-40	3	-	200	400	NO
PC-50	3	-	200	500	NO
PC-60	3	-	200	600	NO
1L-PC-40	3	1	200	400	NO
2L-PC-40	3	2	200	400	NO
4L-PC-40	3	4	200	400	NO
2L-PC-30	3	2	200	300	NO
2L-PC-50	3	2	200	500	NO
4L-PC-60	3	4	200	600	NO
RC-40	3	-	200	400	YES
2L-RC-40	3	2	200	400	YES

Table 7 presents the test matrix and the specimens designation name that will be used throughout this study. PC indicates that the specimen group is made of plain concrete, while RC indicates that transverse steel reinforcement has been added to the specimen. The numbers 30, 40, 50 and 60 specify the specimen height and therefore differentiates among the different slenderness ratios. Also, the abbreviation 1L, 2L and 4L designates the number of confining layers.

3.3.2. Preparation of Column Specimens

3.3.2.1 Concrete Mix

Low strength concrete was used throughout the study. Ready-mix concrete was chosen over the conventional mix because of the large amount of concrete needed and since concrete itself is not the main focus of the study. The only requirement is that the concrete have low strength in order to meet with the loading capacity of the machine.

All the thirty-six columns were cast vertically from one batch of concrete. The specimens were thoroughly vibrated using a rod vibrator. At the same time, small cylinders (150 mm diameter and 300 mm height) were cast in order to monitor the concrete strength at 7, 28 days and at the time of testing of the columns. After 7 days, all specimens were demolded and the cylinders were cured until testing.

Figure 18. Casting of concrete columns.

3.3.2.2. Capping

The top ends of vertically cast cylinders are not usually smooth surfaces, this is mainly due to hydration during concrete setting. Sulfur capping was used in order to provide a smooth and flat surface and to ensure parallel top and bottom surfaces of the cylinders and orthogonal to the loading axis.

3.3.2.3. Epoxy Resin:

The Sikadur®-300 was used. It is a two part, epoxy based impregnating resin. This epoxy resin is typically used for strengthening and rehabilitation of concrete with fiber reinforced polymers. It has excellent adhesion to concrete and most structural material. It has high modulus, high strength impregnating resin.

The mixing ratio is part A: part B =100: 34.5 by weight. Parts A and B are mixed together for approximately 3 minutes at low speed.

3.3.2.4. Hemp fabrics Preparation

In this part of the study, commercial bidirectional hemp fabrics are used instead if raw fibers for their ease of use and lower variability. Fabrics were cut into designated sizes to guarantee wrapping of 1, 2 and 4 layers with an overlap equal to half perimeter. The fabric lengths are presented in table 8. The fabric width depends on the columns height.

Table 8. Hemp fabrics dimensions.

Number of layers	Fabric length (cm)
1	95
2	157
4	283

First, the fabric was saturated with epoxy using a brush. The concrete surface was also coated with epoxy. After impregnation, the fabric was ready for installation.

Figure 19. Fabric and surface preparations.

The saturated fabrics were applied to the columns surfaces by hand, using the wet lay-up technique. When applying the fabric, a slight constant pull was maintained across the width of the fabric in order to ensure a flat adhesion to the concrete and to squeeze out any air pocket. Once the specimen is fully wrapped, a final coat of epoxy was applied mainly at the ends to ensure a complete saturation.

Figure 20. Application of hemp FRP wraps.

3.3.3 Hemp Tensile Test Procedure

The same procedure of tensile testing was done for the hemp fabrics, in order to fully understand the behavior of the hemp-confined columns. The tensile strength of the hemp fabrics epoxy coated strips was tested.

The tensile testing was done using the ASTM D 3822-14 the 'Standard for Tensile Properties of Single Fibers'. Figure 21 shows a hemp fiber rope test setup. (ASTM D 3822-14, 2014)

Figure 21. Tensile test setup for hemp fabrics.

The key testing points are listed below:

1- Gauge length: the selected gauge length, that is the clear distance between the two grips, is 200 mm. This gauge length was kept constant throughout the test. Each strip is 2.5 cm wide and 25 cm long.

   The thickness of 1 layer of hemp is 1.2 mm.

2- Constant rate of extension: the rate of extension or pull was set 1 mm/min for all the tests.

3- Clamps: clamps with flat jaws were used to grip the fiber specimens and minimize

their slippage.

3.3.4. Uniaxial Compression Test Procedure

Four linear variable displacement transducers (LVDTs) were placed on each column. The LVDTs were positioned 90˚ opposite from each other and placed at the mid-height of each cylinder. Axial compression test was done on all samples using an MTS machine with a constant displacement rate of 3 mm/min.

All the specimen were axially compressed up to failure and the results were collected using a data logging system.
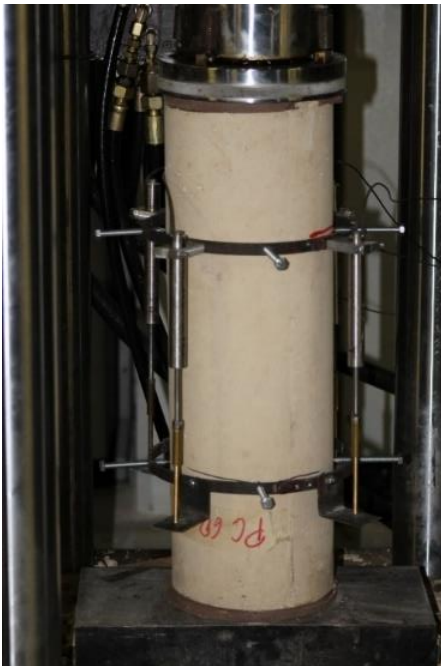
Figure 22. Uniaxial compression test setup.

CHAPTER 4

DISCUSSION OF TEST RESULTS AND ANALYSIS

4.1. Hemp Tensile Test

Hemp fabric strips coated with epoxy were tested in tension up to failure. The results showed a typical load-elongation curve. As the load increases, the fiber extension increases until it reaches a peak stress at a certain point of extension. The load corresponding to the maximum point of extension is the maximum tensile load P_{max} that the fiber can carry. Because hemp fibers are brittle by nature, the fiber broke after reaching the maximum elongation. Similar load-elongation curves were obtained. The stress strain diagrams of three samples were averaged and the modulus of elasticity of the hemp fabrics was therefore calculated.

Figure 23. Hemp fabric tensile strength.

Figure 23 displays the averages stress-strain curve of hemp fiber under tensile load. The modulus of elasticity is 1660 MPa and the ultimate strain is 0.045 mm/mm.

4.2. Test Variable: Number of confining layers

4.2.1. Stress strain relationships

Figure 25 illustrates the axial compressive stress versus the axial strain of the specimens having constant slenderness ratio and different number of confining layers (PC40, 1L-PC40, 2LPC-40 and 4L-PC40)
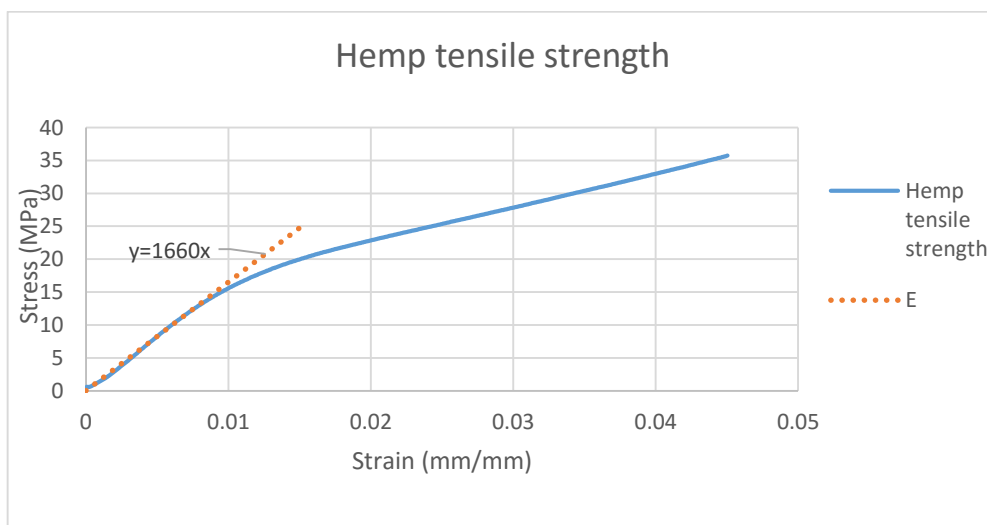
The stress-strain curve of unconfined specimen is similar to conventional stress-strain diagrams of plain concrete cylinders. The curve starts with a linear portion lasting up to approximately 70% of the ultimate load. After this linear part, the curve enters in a non-linear stage where large strains begin to be registered for small increments of loads. The curve nonlinearity is mainly due to the formation of microcracks in the concrete. The ultimate strength is reached when a large crack network is formed from the microcracks. After reaching the ultimate load, any additional load leads to a brittle failure of the specimen.

The stress strain curves of confined specimens can be divided into two linear zone connected by a non-linear transition zone.

The stress strain curves of both confined and unconfined specimens start similarly. The curves start with a purely linear response. Once the maximum compressive strength is attained, the behavior of the confined specimens is no longer similar to the conventional behavior of PC specimens. In this first linear region, the confinement of hemp FRP jacket is

46

not activated since the axial stresses and strains are relatively low and the lateral expansion is insignificant.

When the applied stress approaches the maximum strength of the unconfined specimen, the stress strain curve enters a nonlinear transition zone in which micro cracks are propagated in the concrete core and the lateral expansion increases considerably.

With the increase of the lateral expansion the hemp jacket starts to confine the concrete core and the stress-strain curve enters a second linear region.

This latter linear region is directly dominated by the structural behavior of the confining layer. The hemp confinement is fully activated. A change in the color of the hemp fibers is noticed in this region, indicating the stretching that the material undergoes.
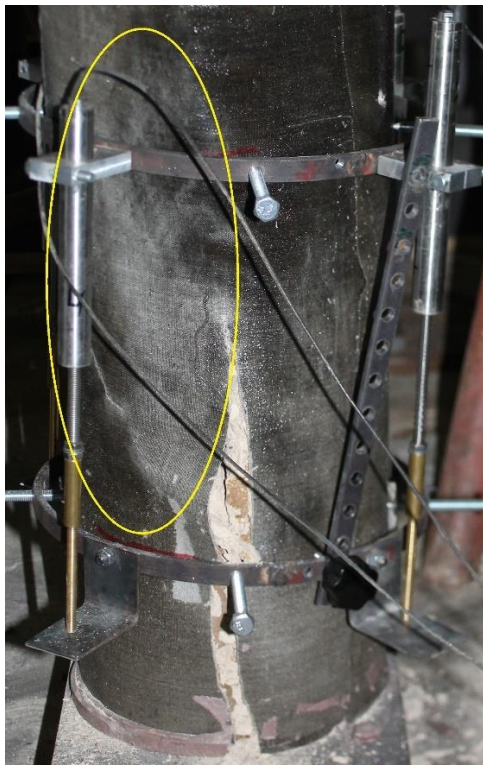
Figure 24. Stretching of the hemp wraps.

In this region, the stress strain curve starts to drop at a slow rate. Unlike the unconfined specimen, there is no sudden failure of the specimen. All specimens had a descending post-peak branch. However, the slope of the descending branch decreases with the increase of the number of confining layers.

Once the maximum tensile strength in the hemp is exceeded, the hemp jacket ruptures with a loud popping noise.
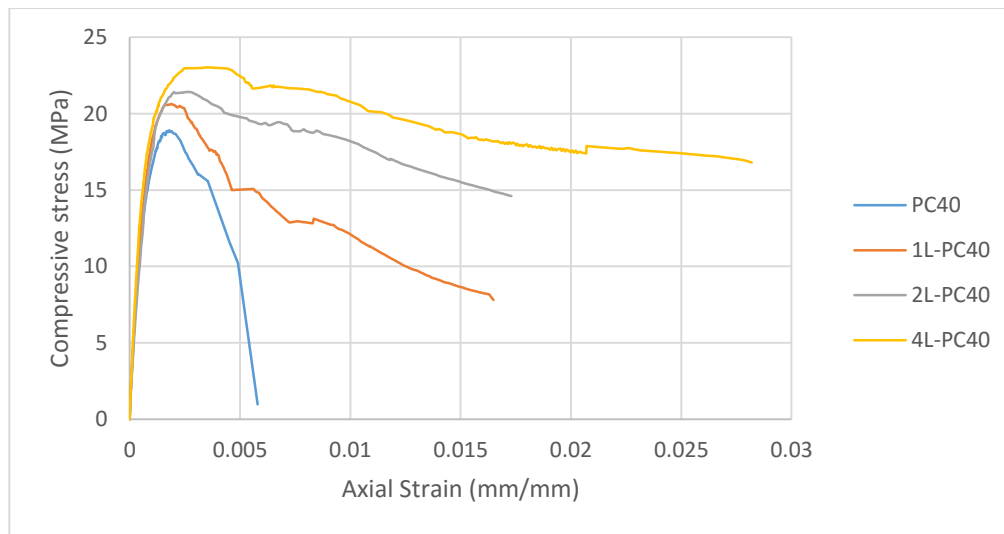
Figure 25. Stress-strain curves of specimens with different number of confining layers.

Based on Lam and Teng, the post-peak behavior of the stress-strain curve of a concrete specimen depends on the confinement ratio. In their research, they adopted the confinement ratio criterion of 0.07 suggested by Spoelstra and Monti. If this confinement ratio is greater than 0.07 the post-peak branch is ascending; if the latter ration is smaller than 0.07 the post-peak branch is descending and the confinement is considered insufficient. On the other hand, Mirmiran et al. used a confinement ration criterion of 0.15.

However, these criterions are based on the results of concrete confined with synthetic fibers. The applicability of these criterions is questionable with the use of natural fibers that have lower mechanical properties than the synthetic fibers.(Lam & Teng, 2003)

Three types of stress-strain curves are illustrated in figure 25. The first stress-strain curve type is the conventional curve of unconfined concrete with a brittle failure of the specimen. The second type of stress-strain curve is noticed for the specimen confined with 1 layer and 2 layers with confinement ratios of 0.017 and 0.035 respectively. The stress-strain curve of these specimen is a typical curve of confined concrete with a descending post-peak branch; also, the stress corresponding to the ultimate strain (strain at failure) is smaller than the compressive strength of concrete. As the number of confining layers increases the slope of the descending post-peak branch decreases. Finally, the specimen confined with 4 layers of hemp maintained a smaller descending slope and failed at a stress level approximately equal to the compressive strength of unconfined concrete. The confinement ratio of the specimens wrapped with 4 layers is 0.102.

When the confinement ratio increased to a value greater than the criterion given by Lam and Teng, which is a confinement ratio of 0.07, the stress-strain curve shifted from a typical insufficient confined type to a sufficient confined one. However, this increase in the confinement ratio did not lead to an ascending post-peak branch. (Lam & Teng, 2003)

The maximum number of confining layer considered in this study is 4 layers with maximum confinement ratio of 0.102. This value of concrete confinement is still smaller than the criterion of 0.15 given by Mirmiran et al. It is therefore recommended to increase the confining ratio by increasing the number of confining layers and monitor the confining ratio that will lead to an ascending post-peak behavior. (Mirmiran et al., 1998)

It is important to point out here that one confined sample with 4 layers showed an unexpected stress strain curve. This kind of error is attributed to an error during the experiment. The LVDTs readings were restrained. In this study, the stress-strain of this latter specimen is eliminated since to have reasonable data.

4.2.2. Confinement performance:

Table 9 summarizes the confinement performance of hemp fibers with the increase in the number of confining layers. The confinement effectiveness $\frac{f'_{cc}}{f'_{co}}$ increases with the increase of the number of confining layers. The confinement effectiveness increased by 9.1%, 13.3% and 21.7% for the specimens confined with 1 layer, 2 layers and 4 layers respectively. The axial strain ratio also increased. The axial stain ratio increase by 5.6%, 12.2% and 93.3% for the specimens confined with 1 layer, 2 layers and 4 layers respectively.

Table 9. Average test results of the specimens with different number of confining layers under uniaxial compression test.

Specimen type	f'_{co}	ε_{co} (%)	f'_{cc}	ε_{cc} (%)	f_l	$\frac{f_l}{f'_{co}}$	$\frac{f'_{cc}}{f'_{co}}$	$\frac{\varepsilon_{cc}}{\varepsilon_{co}}$
PC40	18.91	0.18	-	-	-	-	-	-
1L-PC40	-	-	20.64	0.19	0.33	0.017	1.09	1.056
2L-PC40	-	-	21.43	0.202	0.69	0.035	1.13	1.122
4L-PC40	-	-	23.03	0.348	1.94	0.102	1.22	1.933

4.2.3. Ductility of hemp FRP confined concrete

Ductility is defined as the ability of a structural system or element to undergo prior to collapse inelastic deformation without substantial loss in resistance.

In reinforced concrete structures, steel reinforcement tends to offer the ductility to the structural member unlike concrete material that has relatively low tensile strength and ductility. Also, in conventional reinforced concrete structures, ductility is defined as the ratio of the ultimate deformation that the structural member undergoes to the yield deformation.

However, this concept cannot be used in calculating the ductility of hemp FRP confined structural element. Unlike steel fibers in which great amount of inelastic deformation happens once the steel starts to yield; hemp fibers are elastic up to failure. Hemp fibers do not have yielding characteristics as shown in figure 23 and therefore no plastic work is involved.

From here the necessity to find a suitable approach that can reflect the enhancement in ductility due to the confinement of concrete with hemp fibers.

One way of addressing this issue is to compare the fracture energy of unconfined plain concrete and hemp FRP confined specimens.

Fracture energy is defined as the amount of energy absorbed by the specimen while breaking; this value is equal to the area under the load-displacement curve. The load and displacement being in unit of KN and mm respectively lead to a fracture energy unit of Nm.

Another way of evaluating the enhancement in ductility is to calculate the axial strain ratio of the hemp FRP confined specimens to the unconfined control specimen. The

axial strain used in this method is the axial strain corresponding to the maximum load. The axial strain ratio is used mainly when the stress-strain curve features an ascending post peak branch where the peak stresses and strains are attained simultaneously.

Table 10 gives the average fracture energy and the ductility indices of the specimens with different number of confining layers. In all considered cases, significant enhancement in ductility is noticed. The ductility index increases with the increase of the number of confining layers. The ductility index of specimens confined with 1, 2 and 4 layers are 2.78, 3.95, 6.98 respectively. This indicates that the area under the load-displacement increases with the increase of number of confining layers. Therefore, more energy is absorbed by the specimen and more energy is needed to damage the specimen and to rupture the hemp jacket. Hence, the increase of the number of confining layers results in an increase of both the energy absorption capacity and ductility of the hemp confined specimen.

Table 10. Average fracture energy and ductility index of the specimens with different number of confining layers.

Specimen types	Fracture energy (Nm)	Ductility index
PC40	486.76	1
1L-PC40	1353.04	2.78
2L-PC40	1923.21	3.95
4L-PC40	3397.89	6.98

4.2.4. Failure mode

The failure modes of the PC specimens and the specimens with different number of confining layers are shown in figure 26,

The confined samples failed by the formation of a sudden single crack in the confining layer accompanied with a loud popping noise, indicating the brittle behavior of the hemp fibers. The crack formed is a straight fracture crack parallel to the axial stress direction and perpendicular to the orientation of the hemp fibers of the confining layers.

The concrete core of the confining layer is fully crushed indicating that the failure of the concrete happened before the rupture of the hemp confining layers. The confinement is activated due to lateral expansion once the concrete core has cracked.

The hemp FRP confining layer could not be removed, indicating a strong bond between the confining layer and the concrete core. It was observed that the concrete core is split into two halves in most of the specimen. Also it was noticed that the crack fracture for the specimens confined with 4 layers is throughout the whole sample whereas for the specimen confined with 1 and 2 layers the crack stopped almost at three quarters of the specimen height as shown in figure 26. This crack pattern may be due to the increase of the fracture energy; that is the increase of energy absorbed to damage the specimen; with the increase of the number of confining layers.

It is important to outline that the failure of hemp FRP confined specimens is different from the failure modes exhibited by specimens confined with synthetic fibers such as carbon and glass FRP. The typical failure modes of GFRP and CFRP is shown in figure 26(e).
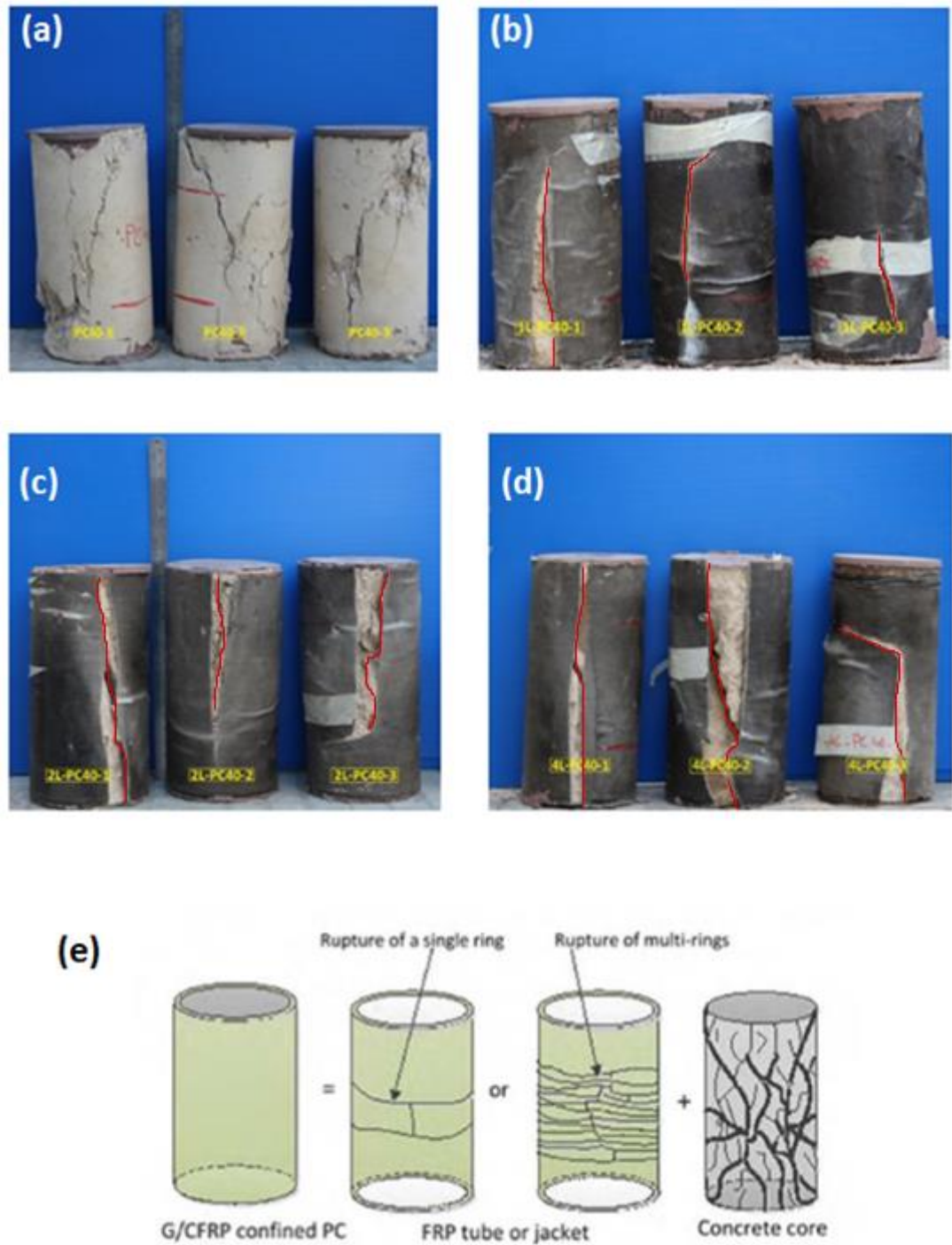
Figure 26. Failure modes (a) PC40, (b) 1L-PC40, (c) 2L-PC40, (d) 4L-PC40, (e) schematic illustration of synthetic GFRP and CFRP failure modes.

This difference in the failure mode may be due to the difference of the tensile properties of the natural and synthetic fibers.

4.2.5. Prediction of ultimate axial stresses and strains

Table 11 presents the existing confinement models used to predict the maximum axial compressive strength of circular FRP confined concrete.

The ACI model presented is based on the existing test data of confined concrete with synthetic fibers mainly glass and carbon. The ACI used the same model presented by Lam and Teng with a confinement effectiveness coefficient of 3.3. This model is applicable for compression member with f_c' less than 70 MPa.

The model presented by Wu and Zhou is developed based on Hoek-Brown failure criterion. The Hoek-Brown criterion is an empirical failure criterion derived from rock mechanism; it predicts the strength based on the principal stresses. Wu and Zhou proposed a similar relation and transformed all the rock material dependence parameters to plain concrete dependence, for concrete stengths varying between 18 and 80 MPa.

Kono et al linearly related the maximum confined strength of concrete to plain concrete strength multiplied by the confinement pressure.

The models presented by the ACI and Wu and Zhu gave approximately same predictions. The predictions given are acceptable for low number of confining layers. The percentage error increases with the increase of the number of confining layers.

Table 11. Strength models for circular columns.

Reference	Equations
(ACI Committee) 440.2R-08	$f'_{cc} = f'_{co} + 3.135 f_l$
(Youssef, Feng, & Mosallam, 2007)	$\dfrac{f'_{cc}}{f'_{co}} = 1 + 2.25\left(\dfrac{f_l}{f'_{co}}\right)^{1.25}$
(Kono, Inazumi, & Kaku)	$f'_{cc} = f'_{co} + 0.0572 f_l f'_{co}$
(Lam & Teng, 2001)	$f'_{cc} = f'_{co} + 2 f_l$
(Wu & Zhou, 2010)	$\dfrac{f'_{cc}}{f'_{co}} = \dfrac{f_l}{f'_{co}} + \sqrt{\left((16.7/f'^{0.42}_{co} - f'^{0.42}_{co}/16.7)\dfrac{f_l}{f'_{co}} + 1\right)}$
(Harries & Kharel, 2002)	$f'_{cc} = f'_{co} + 4.629 f_l^{0.587}$

Also, the models of Youssef et al. and Kono et al. have the same strength prediction but slightly underestimated the confined concrete strength for all cases

The model presented by Harries et al. slightly overestimates the confined concrete strength for all cases.

Lam and Teng model predicts the ultimate compressive strength accurately for all number of confining layers with differences all below 4%. In their model, the confinement efectiveness coefficient of 2 is much is lower than the coefficient used in ACI 440.2R-08. This decrease in the value of the confinement effectiveness coefficient lead to a close

prediction of the ultimate strength of confined concrete even for high number of confining layers.

Table 12. Comparison between current experimental test results and predicted stress of confined concrete with hemp FRP.

	HFRP confined PC					
Models	1L-PC40 f_{cc}'(MPa)	% Diff.	2L-PC40 f_{cc}'(MPa)	% Diff.	4L-PC40 f_{cc}'(MPa)	% Diff.
Test Results	20.64	-	21.43	-	23.03	-
ACI committee	20.39	-1.23	21.86	2.02	24.82	7.76
Youssef et al.	19.33	-6.34	19.91	-7.08	21.29	-7.55
Kono et al.	19.42	-5.91	19.93	-7.00	20.95	-9.03
Lam and Teng	19.85	-3.82	20.79	-2.97	22.68	-1.52
Wu and Zhu	20.45	-0.93	21.93	2.33	24.76	7.52
Harries and Kharel	21.89	6.036	23.38	9.10	25.62	11.27

Figure 27 illustrates the different equations used in the prediction of the confined compressive strength for the different lateral pressures. The experimental values are also plotted on the same graph. Figure 27 confirms that the model presented by Lam and Teng gives the closest predicted values to the experimental values. It is also imperative to indicate that the lowest percentage error between the experimental values and the values predicted using Lam and Teng model is for the specimens confined with 4 layers. These specimens have a confinement ratio greater than 0.07 in accordance with the

recommendation given by Lam and Teng for a better predicition of the confined
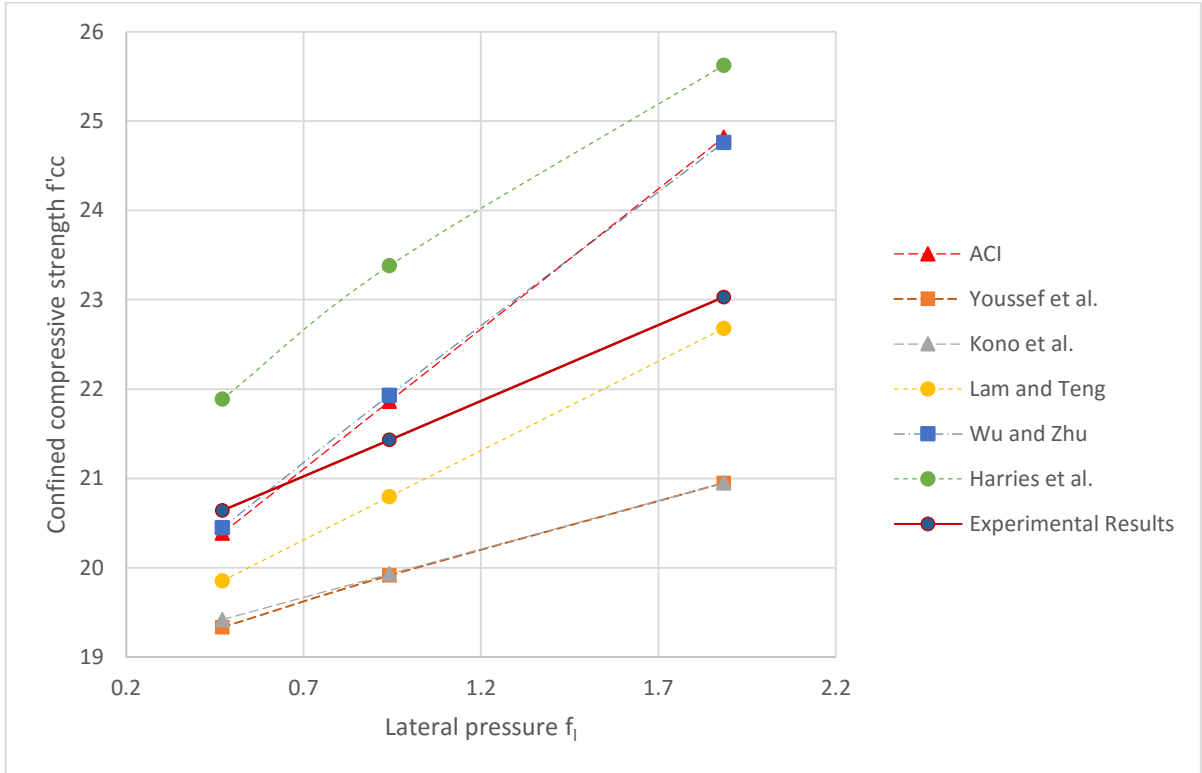
compressive strength.

Figure 27. Predicted confined compressive strength using existing stress models.

4.2.6. Stress Model

The confinement effectiveness ratio $\frac{f'_{cc}}{f'_{co}}$ values versus the ratio of the maximum

confining pressure to the unconfined compressive strength is shown in figure 28. The

ultimate strength of the confined specimens where normalized based on the ultimate

strength of the unconfined specimens. As shown in figure 28, a linear regression model is

fitted. No tranformation is needed in order to normalize the data. A good correlation is noted with $R^2 = 0.8$.

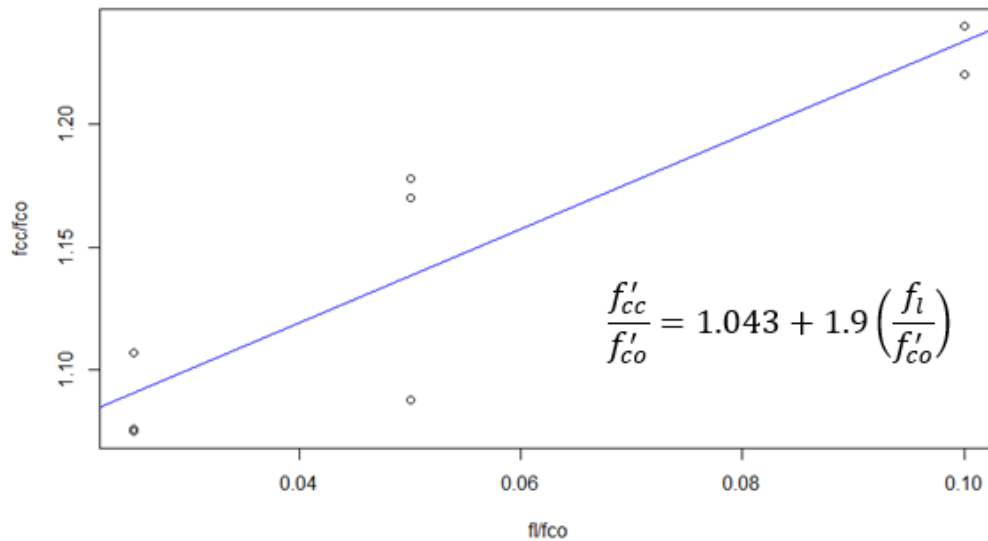$$\frac{f'_{cc}}{f'_{co}} = 1.043 + 1.9(\frac{f_l}{f'_{co}})$$

Figure 28 Linear regression model for the confinement effectiveness vs. confinement ratio.

As expected, this linear model is very close to that presented by Lam and Teng.

4.2.7. Strain models

Also strain models also exist in the literature. The strain models predict the ultimate strain that the confined specimen undergoes. The ultimate strain is the strain corresponding to the maximum compressive strength f'_{cc}.

Table 13. Strain models for circular columns.

Reference	Equations
(Harries & Kharel, 2002)	$\dfrac{\varepsilon_{cc}}{\varepsilon_{co}} = 0.46 + 6.21 \left(\dfrac{f_l}{f'_{co}}\right)^{0.7}$
(LB. Yan & Chouw, 2012)	$\dfrac{\varepsilon_{cc}}{\varepsilon_{co}} = 2.14 + 3.65 \left(\dfrac{f_l}{f'_{co}}\right)$

Table 13 shows a comparison between the experimental values and the theoretical values of the strain models. Both models do not give accurate predictions of the ultimate axial strain. However, the model presented by Yan and Chouw gave better predictions than the model of Elsanadedy.

The model of Yan and Chouw is based on the confinement of concrete with natural flax fiber. The use of natural fibers and therefore approximately comparable material properties may be the cause of the better prediction of the ultimate strain. The model presented by Elsanadedy et al. is based on concrete specimens confined with carbon fiber that have tensile moduli that are much larger than those of natural hemp fibers. This difference in FRP material and properties may lead to this overestimation in predicting the ultimate strain for the concrete specimens confined by hemp fibers using Elsanadedy et al. model.

Also, these models are based on stress-strain curves that have an ascending post-peak branch. This stress-strain behavior is different from the stress-strain behavior of the hemp confined specimens that have a descending post-peak branch. In the case of the

model presented by Elsanadedy et al. the percentage difference between the theoretical and experimental values decreases with the increase of the number of confining layer. As the number of the confining layers increases the stress-strain curve tends to change from a descending post-peak branch to an ascending post-peak behavior and strain model is therefore applicable.

Table 14. Comparison between experimental and predicted ultimate strains of confined concrete with hemp FRP.

	HFRP confined PC					
	1L-PC40	% Diff.	2L-PC40	% Diff.	4L-PC40	% Diff.
Models	ε_{cc} (%)		ε_{cc} (%)		ε_{cc} (%)	
Test Results	0.19	-	0.20	-	0.35	-
Yan et al.	0.17	-12.05	0.22	8.79	0.30	-12.27
Elsanadedy et al.	0.40	111.35	0.42	106.90	0.45	29.50

4.3. Test Variable: Column slenderness ratio

Column length to diameter ratio is considered one parameter that can affect the strength of the column due to secondary moments and slenderness effects.

A total of 24 samples made of plain concrete were tested under uniaxial compression test in order to check the effect of the confinement effectiveness. The slenderness ratios considered in this study are: 1.5, 2, 2.5 and 3. The samples diameter were

held constant, while the samples lengths were varied. All 24 samples were confined with 2 layers of hemp fabric.

All specimens were made using the same concrete ready mix. All the cylinders were instrumented at their midheights with four LVDTs placed at 90° opposite from each other.
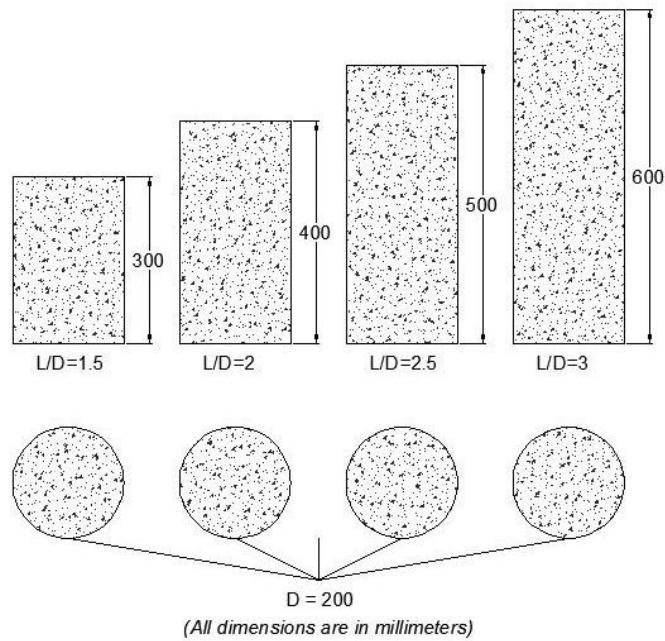

Figure 29. Schematic representation of the specimens with different slenderness ratios.

4.3.1. Failure mode

A typical failure was observed. The failure modes of the PC specimens and the specimens with different slenderness ratios are shown in figure 30?

Similar to the samples confined with different number of layers, the confined samples with different slenderness ratios failed by the formation of a sudden single crack in the confining layer accompanied parallel to the axial direction of loading with a loud popping noise.
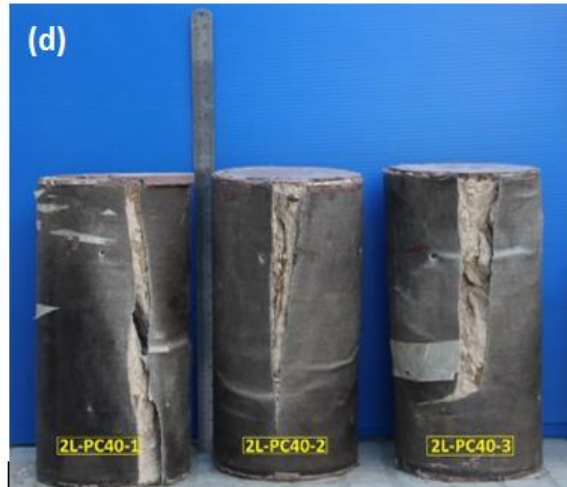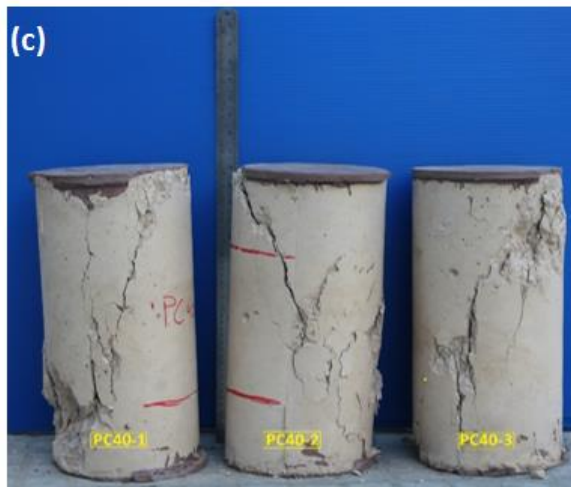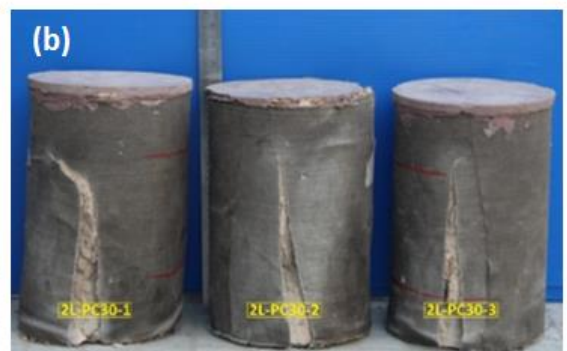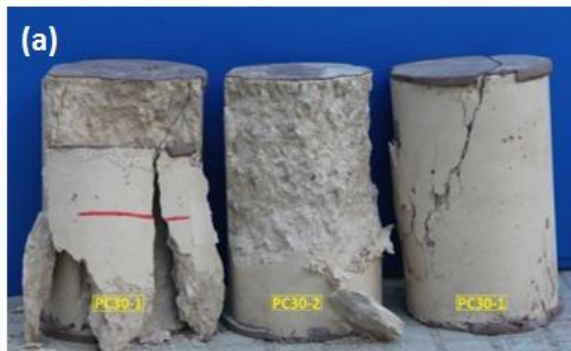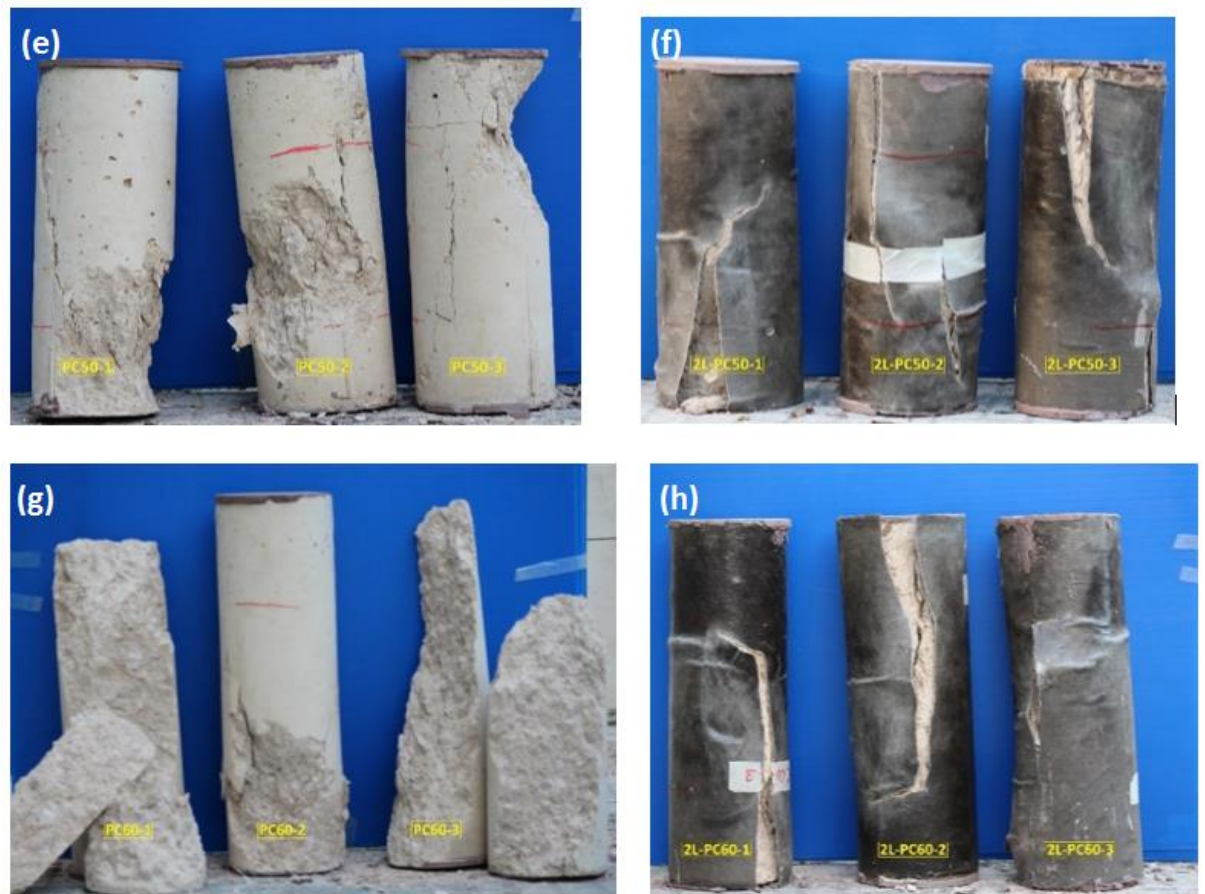
Figure 30. Failure modes (a) PC30, (b) 2L-PC30, (c) PC40, (d) 2L-PC40, (e) PC50, (f) 2L-PC50, (g) PC60, (h) 2L-PC60.

The concrete core of the confining layer is fully crushed indicating that the failure of the concrete happened before the rupture of the hemp confining layers. The confinement is activated due to lateral expansion once the concrete core has cracked. The hemp FRP confining layer could not be removed, indicating a strong bond between the confining layer and the concrete core. It is also important to notice that unlike specimens confined with synthetic fibers, the samples confined with hemp fibers did not fail by debonding.

4.3.2. Comparison between confined specimen with different slenderness ratios

Figure 31 shows the stress strain diagrams of confined concrete with varying slenderness ratios and constant number of confining layers.
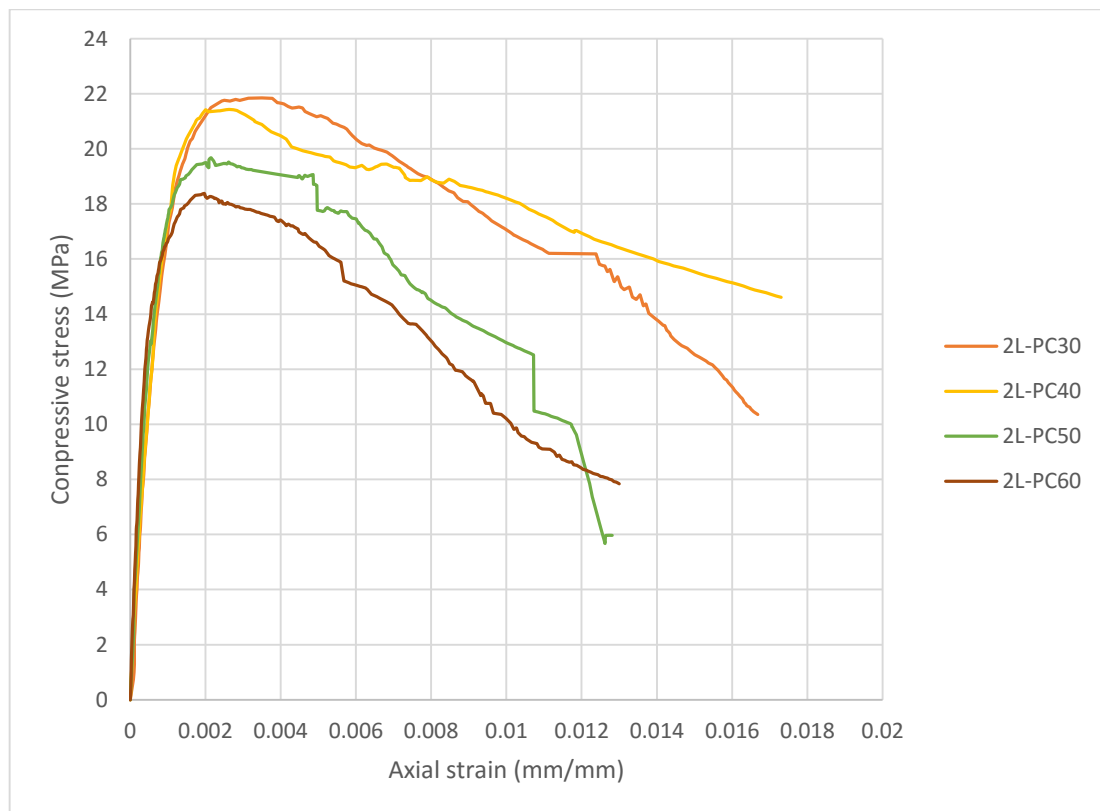

Figure 31. Stress-strain curves of confined specimens with different slenderness ratios.

4.3.2.1. Effect of the slenderness ratio on the ultimate strength

All the results are compared with the standard size cylinder having a slenderness ratio of 2. The ultimate stresses reached by the hemp FRP confined columns were influenced by the column slenderness ratio. All the specimen started linearly with the same slope, but reached different unltimate strengths. The ultimate strength decreases with the increase of the slenderness ratio. The average ultimate strengths are 22.03, 21.43, 19.67 and 18.38 for the slenderness ratios 1.5, 2, 2.5 and 3 respectively. Table 15 shows the decrease of the ultimate strengths with the increase of the slenderness ratios.

Table 15. Average test results of confined specimens with different slenderness ratios under uniaxial compression test.

L/D	f'_{cc}	$\dfrac{f'_{ccn}}{f'_{cc2}}$	ε_{cc} (%)	$\dfrac{\varepsilon_{ccn}}{\varepsilon_{cc2}}$
1.5	22.03	1.03	0.35	1.33
2	21.43	1	0.26	1
2.5	19.67	0.92	0.21	0.81
3	18.38	0.6	0.196	0.745

4.3.2.2. Effect of the slenderness ratio on the ultimate strain

The ultimate strain is the strain corresponding to the ultimate strength attained by the specimen. The ratio of the ultimate strain of confined sample to the ultimate strain of

unconfined sample is used as an indicator to the ductility enhancement provided by the confinement; however the use of this ratio is not preferable since the stress-strain curves have a descending post-peak branch. Table 15 lists the average ultimate strains of the samples with different slenderness ratio. It is noticeable that the ultimate strain decreases with the increase of the slenderness ratio, indicating therefore a decrease in ductility. The ultimate strains are 0.0035, 0.0026, 0.0021 and 0.00196 for the slenderness ratios of 1.5, 2, 2.5 and 3 respectively.

4.3.2.3. Effect of the slenderness ratio on specimen ductility

The effect on the ductility is interpreted by comparing the specimen modulus of toughness measured in units of MPa. The specimen modulus of toughness is the entire area under its stress strain curve. As shown in figure 31, the area under the stress strain curve decreased with the increase of the slenderness ratio above the value of 2. There is no significant difference between the ductility of the specimen with slenderness ratio of 1.5 and 2.

This decrease in ductility is also noted for the unconfined specimens. The area under the stress-strain curve of the unconfined specimens decreases with the increase of the slenderness ratio.

Increasing the slenderness ratio of the column specimens significantly affects the ductility and strength of the wrapped and control specimen. This reduction in strength and ductility is due to buckling instabiity of slender columns.

Table 16. Modulus of toughness and ductility indices of specimens with different slenderness ratios.

	Control Specimens		Confined Specimens	
L/D	Modulus of Toughness (MPa)	Ductility index	Modulus of Toughness (MPa)	Ductility index
1.5	0.084	1.083	0.29	0.947
2	0.0775	1	0.306	1
2.5	0.0562	0.725	0.192	0.628
3	0.0327	0.422	0.176	0.575

Control specimens with slenderness ratios of 2.5 and 3 decreased by 27.5% and 57.8% respectively, whereas the ductility index of the hemp FRP wrapped columns with slenderness ratios of 2.5 and 3decreased by 37.2% and 42.5% when compared to the standard size cylinders having slenderness ratio of 2.
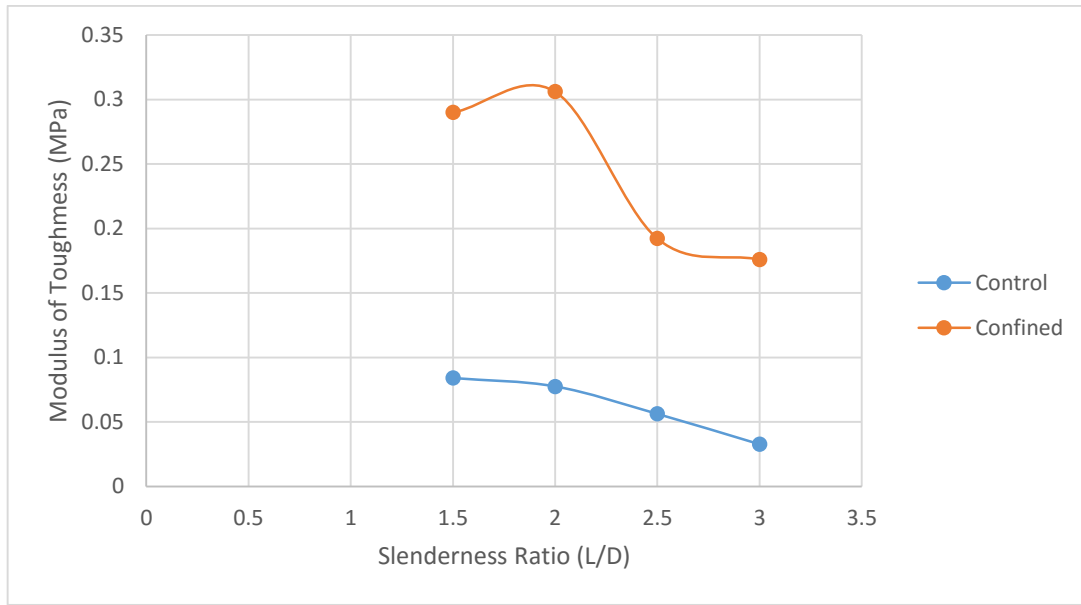
Figure 32. Modulus of toughness versus slenderness ratio for unconfined and confined specimens.

4.3.3. Prediction of confined strength based on slenderness ratio

Existing studies predict the ultimate strengths of FRP confined columns with different slenderness ratios based on the ultimate strength of the specimens having a slenderness ratios of 2. The available models are also parabolic equations.

$$\frac{f'_{ccn}}{f'_{cc2}} = 0.0079 \left(\frac{L}{D}\right)^2 - 0.1030 \left(\frac{L}{D}\right) + 1.1699 \quad \text{(Elsanadedy et al., 2012)}$$

$$\frac{f'_{ccn}}{f'_{cc2}} = 0.0288 \left(\frac{L}{D}\right)^2 - 0.263 \left(\frac{L}{D}\right) + 1.418 \quad \text{(Sadeghian et al., 2009)}$$

Table 17. Comparison between experimental and predicted stresses of confined concrete based on the slenderness ratios

	Models					
L/D	Sadeghian et al.	Experimental	% Diff	Mirmiran et al.	Experimental	% Diff
1.5	22.14	22.03	+0.5	23.32	22.03	+5.8
2.5	20.50	19.67	+4.2	20.15	19.67	+2.4
3	19.97	18.38	+8.65	19.03	18.38	+3.5

The two models presented by Sadeghian et al. and Mirmiran et al. predicts the ultimate compressive strength accurately for the available slenderness ratios. The model presented by Mirmiran et al. gave better predictions for higher slenderness ratio. The percentage difference between the experimental and theoretical values increases with the increase of the slenderness ratio in the model of Sadeghian et al.

The normalized ultimate strength $\frac{f'_{ccn}}{f'_{cc2}}$ versus the slenderness ratio (L/D) is shown in figure 33 The ultimate strength of the slender specimen where normalized based on the ultimate strength of the confined samples with a slenderness ratio of 2. As shown in figure 33, a parabolic equation is fitted to the normalized data by regression analysis. A good correlation is noted with $R^2 = 0.8$.
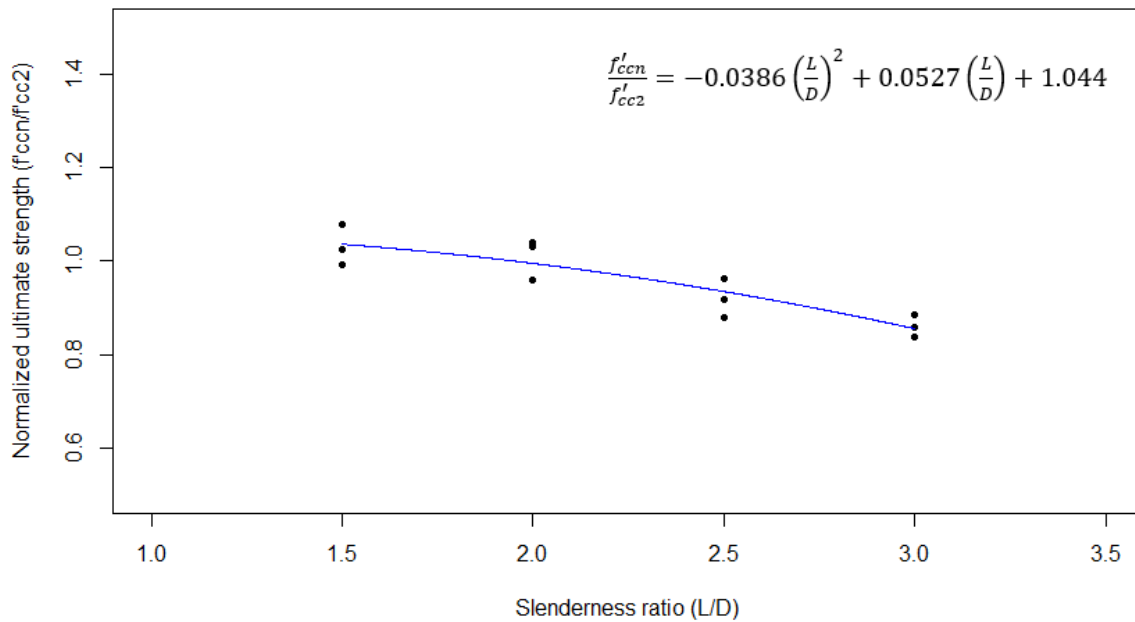
Figure 33. Normalized ultimate strength vs. slenderness ratio

$$\frac{f'_{ccn}}{f'_{cc2}} = -0.00386\left(\frac{L}{D}\right)^2 + 0.0527\left(\frac{L}{D}\right) + 1.044$$

4.3.4. Comparison between confined and control specimen with different slenderness ratios

The confinement effectiveness is also checked for the samples with different slenderness ratio. It is crucial to compare the specimens with different slenderness ratio

with the unconfined samples having the same slenderness ratio. Also, the existing stress

models apllicability is checked for the slender columns.

Figures 34, 35, 36, and 37 illustrate the stress-strain curves of the confined and

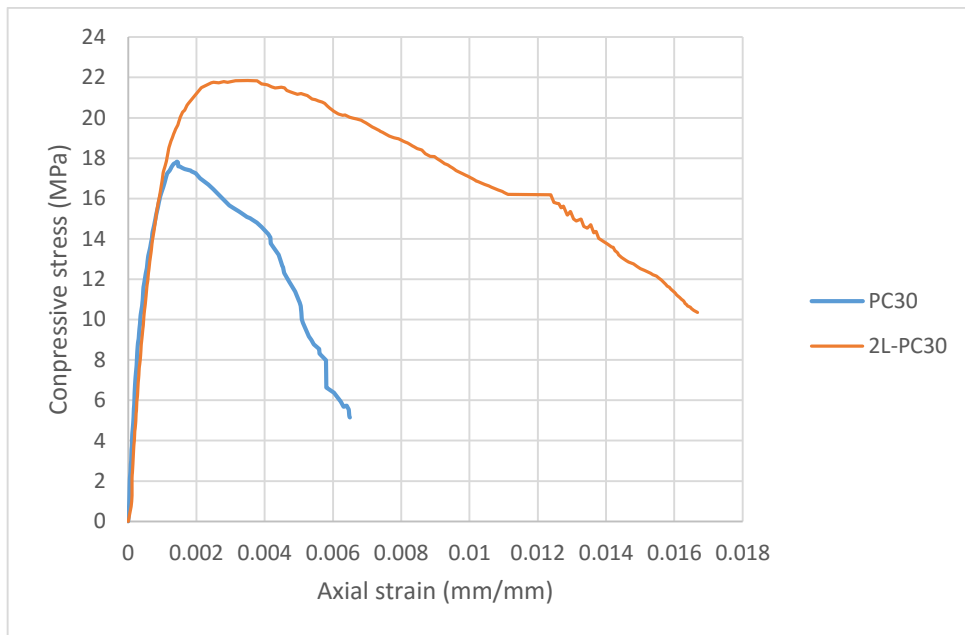unconfined samples with different column slenderness ratios.

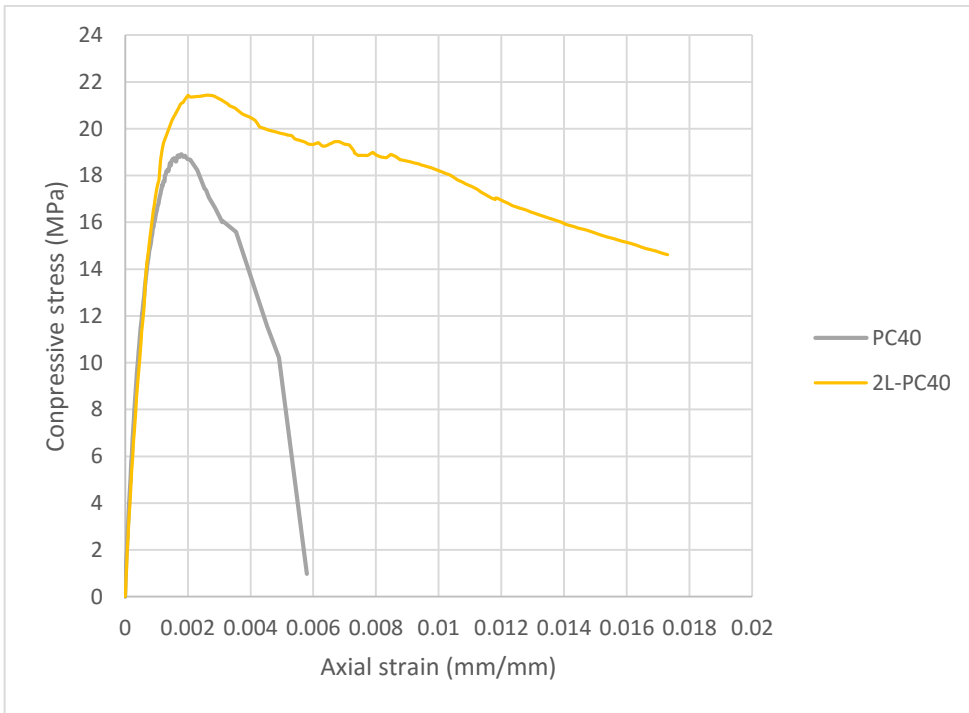
Figure 34. Stress-strain curve of PC30 and 2L-PC30

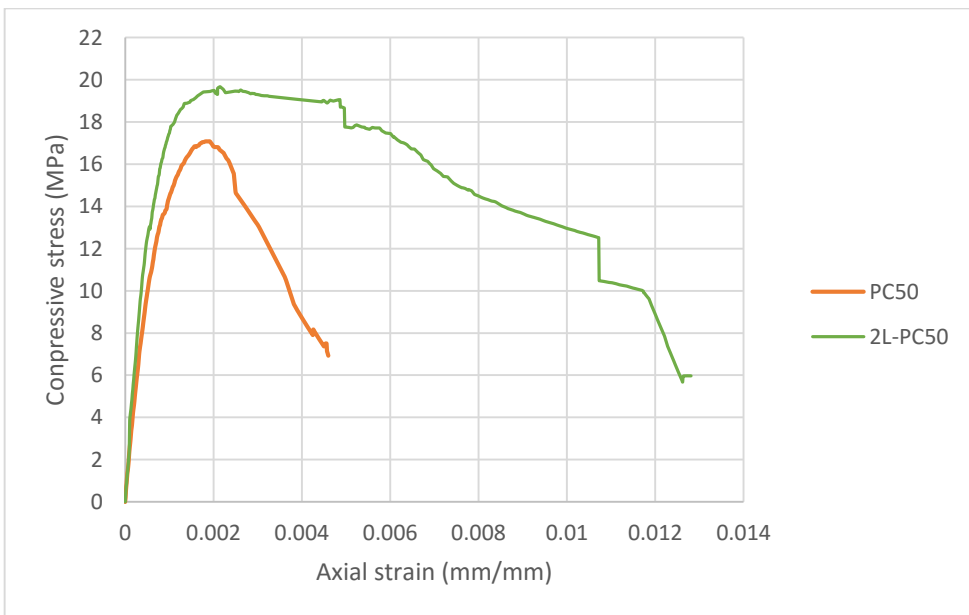Figure 35. Stress-strain curve of PC40 and 2L-PC40

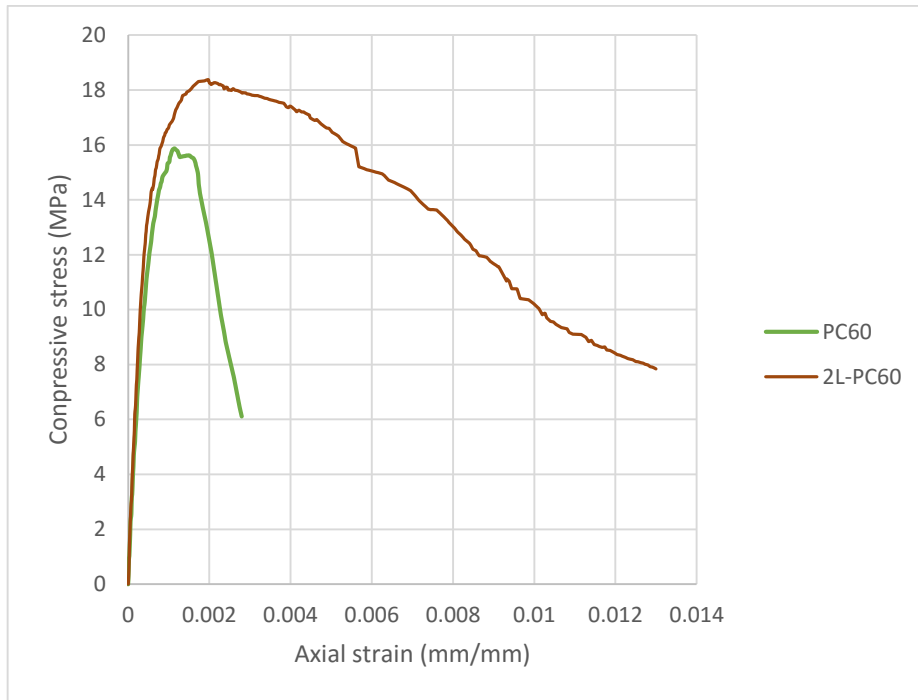Figure 36. Stress-strain curve of PC50 and 2L-PC50

Figure 37. Stress-strain curve of PC60 and 2L-PC60

As shown in figures 34, 35, 36 and 37, the confined specimens have a descending post-peak branch indication an insufficient confinement effect. The confinement effectiveness for the samples 2L-PC30, 2L-PC40, 2L-PC50 and 2L-PC60 is 22.6%, 13.33%, 9.9% and 15.85% respectively. There is no trend in the confinement effectiveness of the confined specimens when compared with the unconfined specimens. However, when the slenderness ratio is 2 or more, there are no significant differences in the confinement effectiveness when comparing confined specimens to the unconfined specimens.

Also, as indicated in table 19, the ductility enhancement increases with the increase of the slenderness ratio. This may be due to the more brittle behavior of slender plain concrete cylinders.

Table 18. Average test results of confined and unconfined specimens with different slenderness ratios under uniaxial compression test.

Specimen type	f'_{co}	ε_{co} (%)	f'_{cc}	ε_{cc} (%)	f_l	$\dfrac{f'_{cc}}{f'_{co}}$	$\dfrac{\varepsilon_{cc}}{\varepsilon_{co}}$
PC30	17.83	0.14	-	-	-	-	-
2L-PC30	-	-	21.85	0.35	0.94	1.22	2.44
PC40	18.91	0.18	-	-	-	-	-
2L-PC40	18.91	-	21.43	0.20	0.94	1.13	1.12
PC50	17.89	0.19	-	-	-	-	-
2L-PC50	-	-	19.67	0.21	0.94	1.10	1.12
PC60	15.87	0.11	-	-	-	-	-
2L-PC60	15.87	-	18.38	0.20	0.94	1.16	1.73

Table 19. Modulus of toughness and ductility index for confined and unconfined specimens with different slenderness ratios.

L/D	Modulus of toughness		Ductility index
	Control	Confined	
1.5	0.084	0.29	3.45
2	0.0775	0.3061	3.95
2.5	0.0562	0.1922	3.42
3	0.0327	0.176	5.38

4.3.4.1. Prediction of confined strength of specimens with different slenderness ratio

The existing stress-models are based on experimental values of specimens with typical slenderness ratio of 2. The adequacy of the use of these stress models is checked for specimens having different slenderness ratio, since in practice slenderness ratios of existing columns are larger than 2.

The predicted confined strength of the cylinders with different slenderness ratio is based on the unconfined compressive strength of the unconfined specimens with the same slenderness ratio

Table 20. Comparison between experimental and predicted stresses of confined concrete with different slenderness ratios.

	HFRP confined PC							
Models	2L-PC30	% Diff.	2L-PC40	% Diff.	2L-PC50	% Diff.	2L-PC60	% Diff.
Test Results	21.85	-	21.43	-	19.67	-	18.384	-
ACI committee	20.78	-4.91	21.86	2.02	20.85	5.98	18.822	2.38
Youssef et al.	18.84	-13.76	19.91	-7.09	18.91	-3.87	16.915	-7.99
Kono et al.	17.88	-18.18	18.96	-11.51	17.95	-8.76	15.922	-13.39
Lam and Teng	19.71	-9.80	20.79	-2.96	19.78	0.54	17.752	-3.43
Wu and Zhu	20.89	-4.39	21.93	2.33	20.96	6.54	19.029	3.51
Harries and Kharrel	22.30	2.03	23.38	9.10	22.36	13.68	20.34	10.63

Table 20 presents a comparison between the experimental test results and the predicted results based on existing stress models. The models given by the ACI, Lam and Teng, Wu and Zhu gave good prediction of the confined specimen even for slenderness ratios higher than 2. The model presented by Youssef et al. predicted well the confined strength of the cylinders with a slenderness ratio of 2, but the percentage error increased when the slenderness ratio varied from the typical value of 2.

Therefore, it is acceptable to use the existing stress models for confined cylinders with slenderness ratio different than 2.

4.4. Test Variable: Addition of transverse steel reinforcement.

In real life situations, the confined concrete columns are subjected to two confinement actions: the FRP external confinement and the transverse steel reinforcement internal confinement. Transverse reinforcement is used to restrain the lateral expansion of concrete, enhance the ductility and delay the concrete failure. Concrete confinement is used for rehabilitation purposes.

Almost all codes and available strength models concentrate on the additional compressive strength due to FRP confinement but neglect the effect of the transverse steel reinforcement. In this section, a basic understanding of the additional effect of transverse steel reinforcement on the enhancement of strength and ductility of confined concrete is checked.

Figure 38 shows the stress-strain diagrams of unconfined concrete samples with transverse steel reinforcement, and their average stress strain diagram. It is important to point out here that one unconfined sample with transverse steel reinforcement RC40-1, showed an unexpected drop in the stress strain curve. This kind of error might be attributed to an error during concrete casting or during the experiment. In this study, the stress-strain of this latter specimen is eliminated since it highly affects the data.

Because the two stress-strain diagrams of RC40-2 and RC40-3 peak at different strain levels. The maximum stress level to be used is the average of these two peaks. However, the average stress-strain diagram will only be used for the calculation of the ductility index.
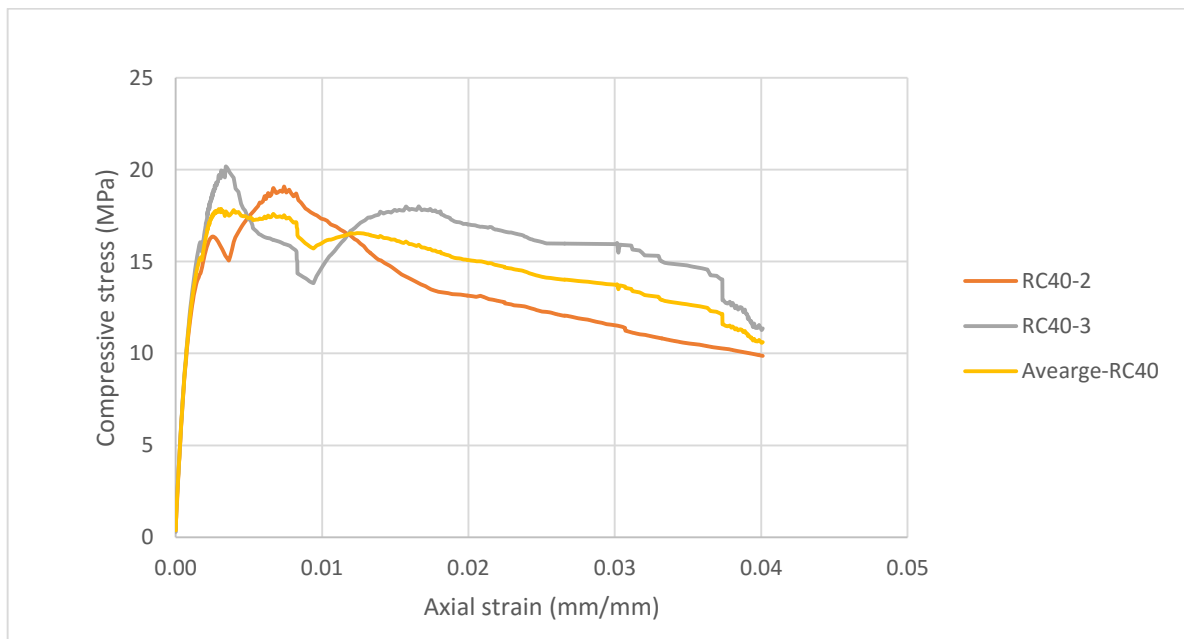

Figure 38. Stress-strain curves of unconfined samples with transverse steel reinforcement.

4.4.1. Confinement effectiveness

The objective of this section is to check the confinement effectiveness provided by the hemp wraps on concrete specimens with transverse steel reinforcement. Table 21 gives the average test results of confined and unconfined specimens with the addition of transverse steel reinforcement. The application of hemp wraps on concrete specimens with transverse steel reinforcement enhanced the compressive strength by 17.3%. In the case of plain concrete, the confinement effectiveness of concrete specimens wrapped with 2 layers of hemp FRP is 13.3%. Therefore, an increase in the confinement effectiveness is noticed when transverse steel reinforcement is added.

Table 21. Average results of unconfined and confined specimens with the addition of transverse steel reinforcement

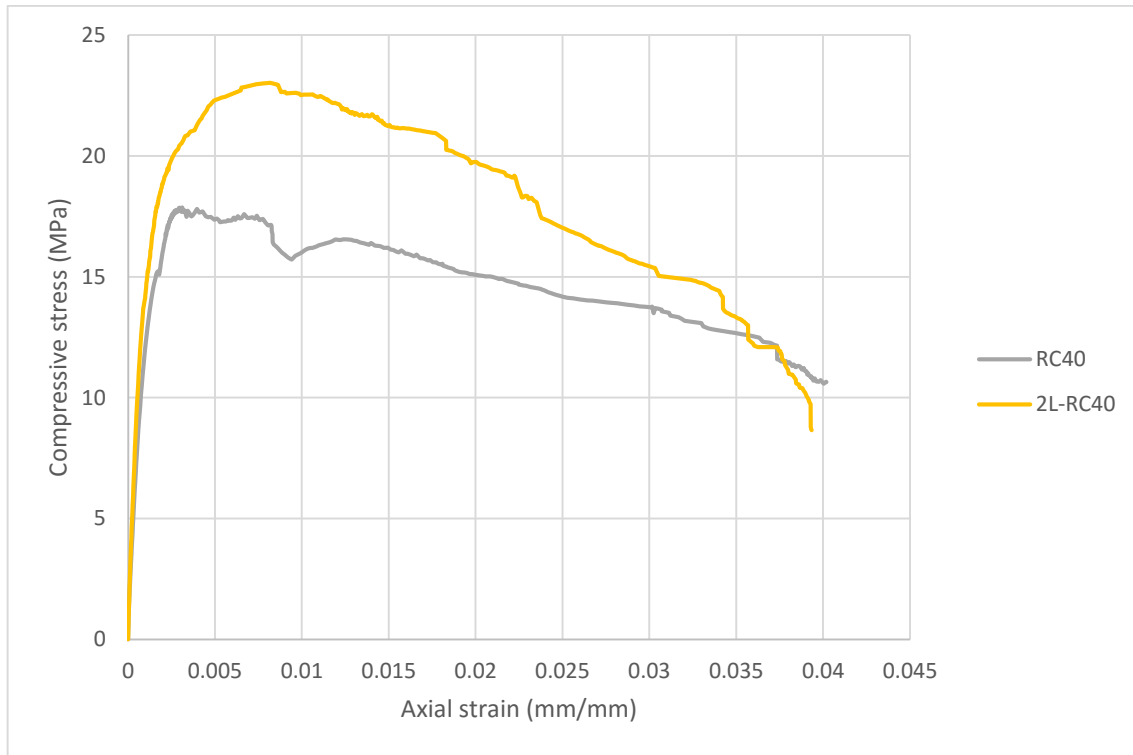| Specimen Type	f'_{co}	f'_{cc}	$\dfrac{f'_{cc}}{f'_{co}}$	ε_{co} (%)	ε_{cc} (%)	$\dfrac{\varepsilon_{cc}}{\varepsilon_{co}}$
RC40	19.63	-	-	0.31	-	-
2L-RC40	19.63	23.02	1.173	-	0.82	2.64

Figure 39. Stress-strain diagrams of unconfined and confined specimen with the addition of transverse steel reinforcement

4.4.2. Ductility enhancement

The ductility indices are calculated using the ratio of the modulus of toughness of the different specimens' type. Table 21 presents the ductility index. In the case of the specimens with transverse steel reinforcement and external FRP confinement, the ductility index is 1.21; whereas in the case of plain concrete, the ductility index is 3.95. This decrease in ductility enhancement is due to the ductility provided by the steel fibers to the control specimens.

Table 22. Modulus of toughness and ductility index of unconfined and confined specimens with the addition of steel reinforcement.

Specimen type	Modulus of toughness (MPa)	Ductility index
RC40	0.59	1
2L-RC40	0.71	1.21

4.4.3. Failure mode

The unconfined samples with transverse steel reinforcement failure is marked by the transverse steel reinforcement hoop rupture accompanied with a loud popping noise. The spiral rupture happens at mid-height of the specimen as shown in figure 40, where the maximum lateral deformation is expected.

Figure 40. Spiral hoop failure

The confined samples with transverse steel reinforcement failure is marked by two stages. The first stage is the formation of a sudden single crack in the confining layer accompanied with a loud popping noise. The crack formed is a straight fracture crack parallel to the axial stress direction and perpendicular to the orientation of the hemp fibers of the confining layers. At this level the specimen did not fail completely, the transverse steel reinforcement is still confining the concrete core. The second stage is the transverse steel reinforcement hoop rupture accompanied with a loud popping noise. The spiral rupture happens at mid-height of the specimen where the maximum lateral deformation is expected.

The concrete core of the confining layer is fully crushed indicating that the failure of the concrete happened before the rupture of the hemp confining layers. The hemp FRP confining layer could not be removed, indicating a strong bond between the confining layer and the concrete core. Figure 41 shows the failure modes of the specimens RC40 and 2L-RC40.
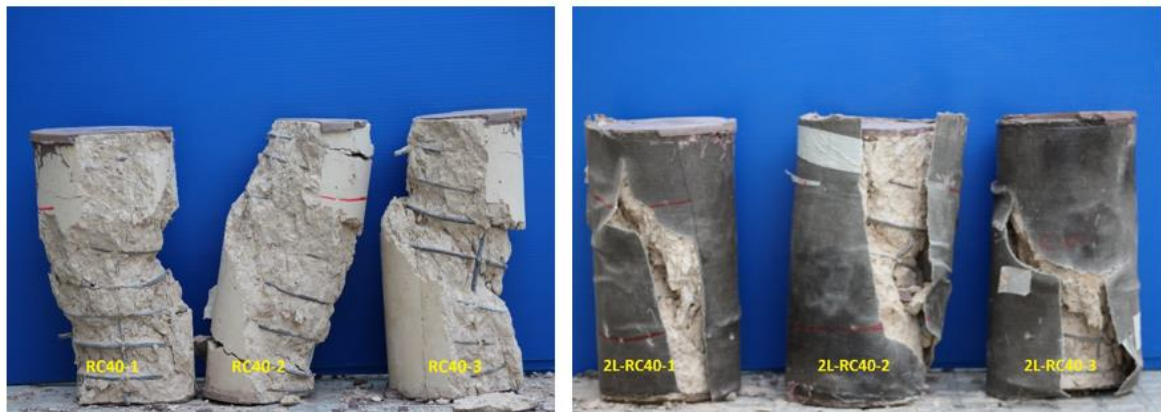

Figure 41. Failure mode (a) RC40, (b) 2L-RC40.

CHAPTER 5

CONCLUSION AND RECOMMENDATIONS

5.1. Conclusion

In this study, the feasibility of the use of hemp FRP as external confinement for concrete has been investigated. Experimental results were presented and compared to stress and strain models collected from the literature.

This study focuses on three parameters that may affect the confinement effectiveness of concrete columns. These parameters are: the number of confining layers, the column slenderness ratio and the addition of transverse steel reinforcement.

The following conclusions can be drawn based on this study:

1- The axial compressive strength and ductility of concrete confined with hemp FRP increases with the increase of the number of confining layers. The axial compressive strength increase for the samples confined with 1, 2, and 4 layers is 9%, 13%, and 22% respectively. The ductility is measured by the fracture energy of the specimens. Thus, an increase in the ductility leads to an increase in the energy absorption capacity. The ductility indices of wrapped confined samples with 1, 2, and 4 layers compared with unconfined samples are 2.78, 3.95, and 6.98 respectively.

2- With the increase of the number of confining layers, two types of stress-strain curves for hemp FRP confined specimens were noticed. The first type is noticed for

the specimens with 1 layer and 2 layers and has an approximate bilinear behavior with a descending post-peak branch and where $f'_{cu} < f'_{co}$. A shift in the stress-strain curve pattern is noticed. The increase of number of layers resulted in a bilinear behavior with a descending post-peak branch with $f'_{cu} \geq f'_{co}$. This type of curve is considered as sufficiently confined. The second type of stress-strain curves is noted for the specimen wrapped with 4 layers of hemp FRP.

3- All specimens with plain concrete core failed by the formation of a single crack of the hemp FRP jacket. The crack is parallel to the axial direction of loading and perpendicular to the fiber orientation. This failure mode is different from the failure of glass and carbon FRP confined columns in which the specimens fail by the debonding of the confining layer.

4- Among all the stress models considered in this study, Lam and Teng predictive model gave the best prediction of maximum confined strength for all the specimens with an error less than 5%.

5- The ultimate stresses reached by the hemp FRP confined columns are influenced by the column slenderness ratio. The ultimate strength decreases with the increase of the slenderness ratio. The ductility enhancement also decreases with the increase of the slenderness ratio and this is interpreted by the reduction of the area under the stress strain curve with the increase of the slenderness ratio above the value of 2.

6- For the case of specimens with transverse steel reinforcement, the specimen confinement leads to an increase in both the axial compressive strength and ductility. The axial compressive strength is enhancned by 17.3%.

7- The confined specimens with additional transverse steel reinforcement lead to a better strength enhancement compared to the case confined plain concrete. However, the addition of transverse steel reinforcement increased the ductility as well but at a smaller rate than the ductility enhacement of confined plain concrete. This decrease in the ductility enhancement is due to the ductility provided by the transverse steel reinforcement as opposed to the brittle behavior of plain concrete.

8- The specimens with added transverse steel reinforcement failed by the formation of a single crack of the hemp FRP jacket followed by the rupture of a spiral hoop. The crack is parallel to the axial direction of loading and perpendicular to the fiber orientation. The failure in the spiral steel reinforcement occurs at mid-height of the specimens where large deformations are expected.

5.2. Recommendations

In order to achieve a sustainable construction, the shift from the use of synthetic FRP confining material to natural bio-based fibers is highly recommended. Extensive research should be done to check the feasibility of this shift. Generally, this experimental study gave promising results concerning the use of natural fibers as construction materials. However, more research should be done to get comparable results with carbon and glass FRP. Therefore, it is recommended to:

1- Increase the number of the confining layers to ensure an ascending post-peak behavior which will lead to confinement performance and will be comparable to the confinement using synthetic fiber. The value of lateral confining pressure indicated

by Lam and Teng (2003) that ensures an ascending post-peak behavior is not applicable in the case oh hemp FRP. Therefore, it is recommended to check the applicability of the criterion given by Mirmiran et al. (1998) which is considered to be more conservative.
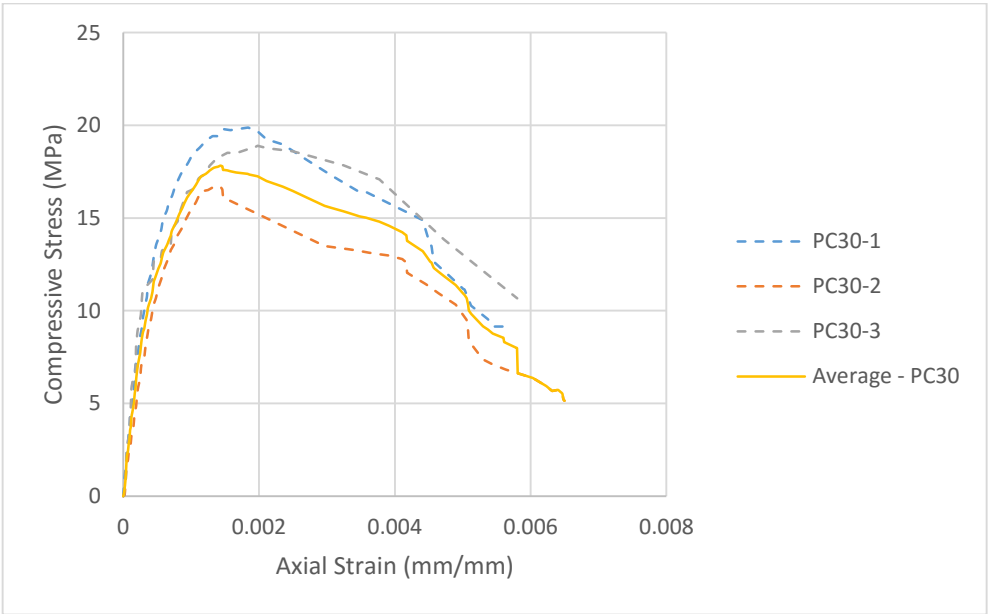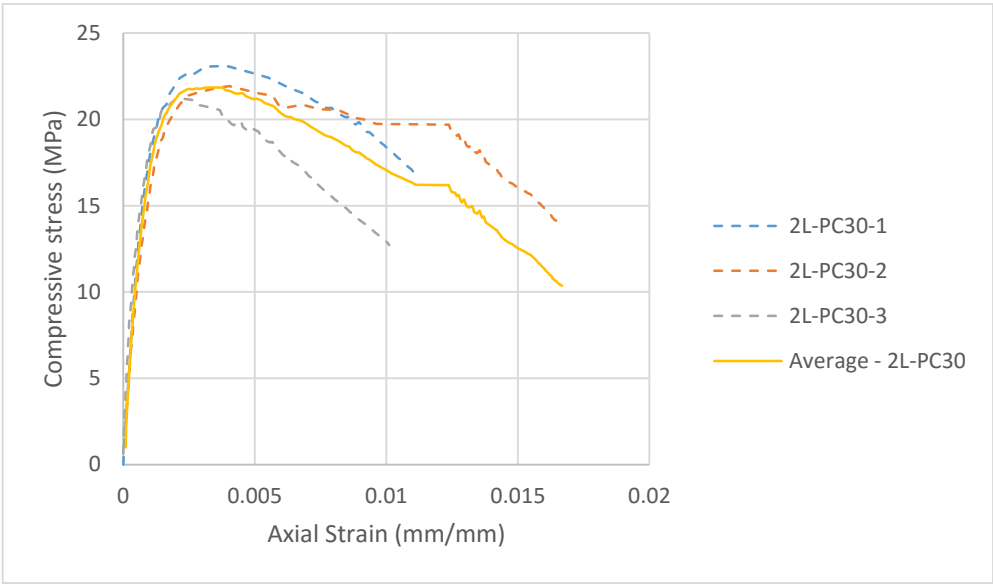
2- Extensive research is also needed on confined reinforced concrete. The effect of the confinement of the addition of transverse steel reinforcement should be further investigated by altering the spacing of transverse ties.
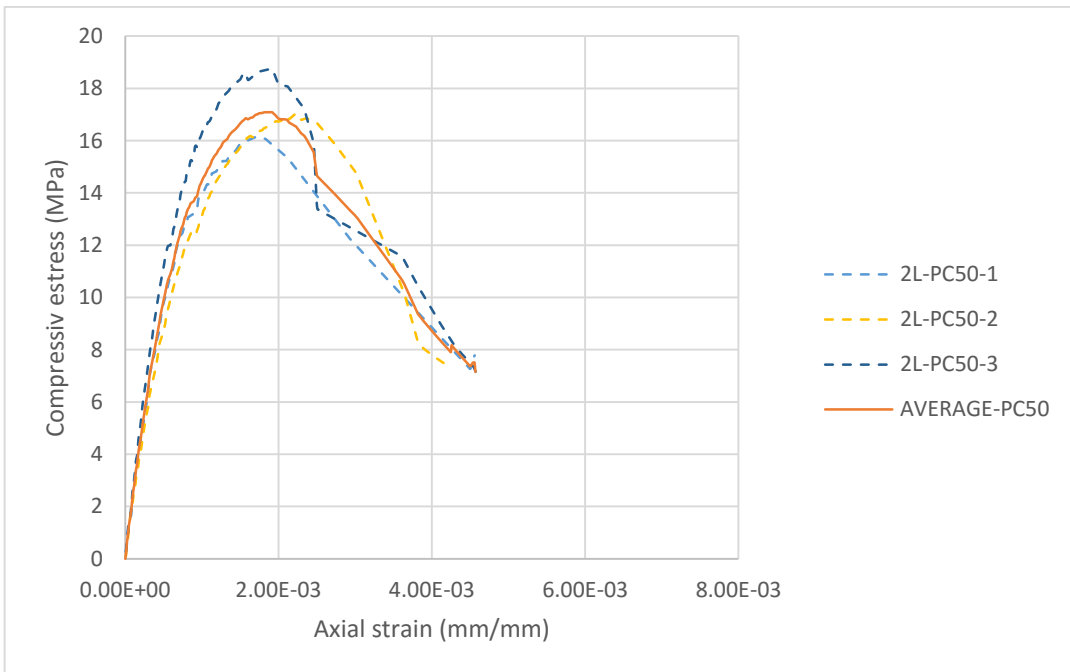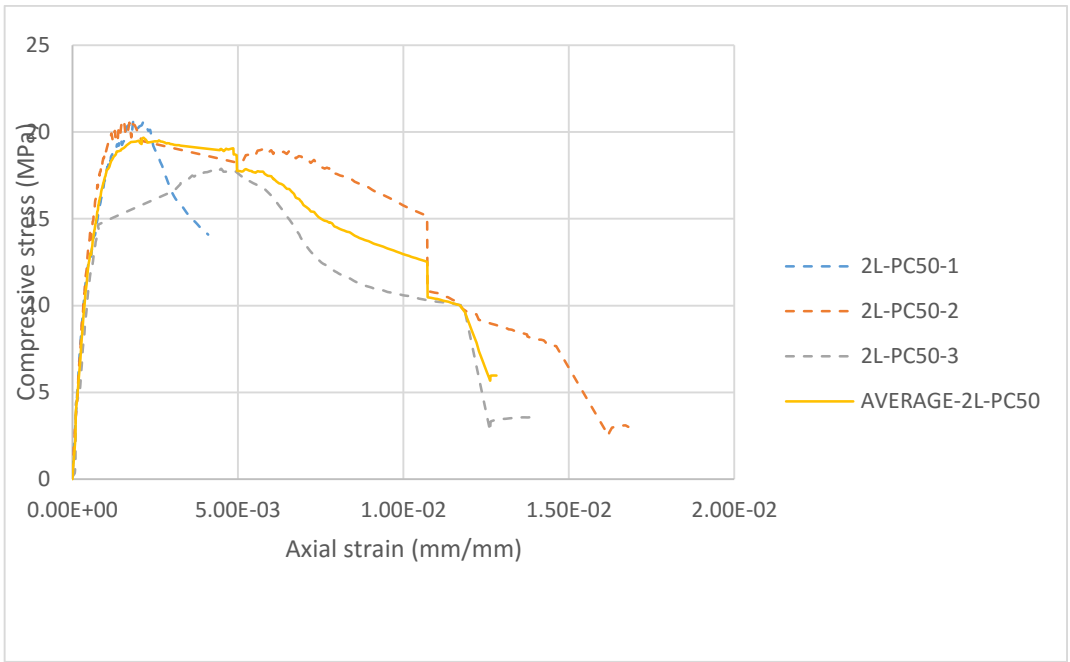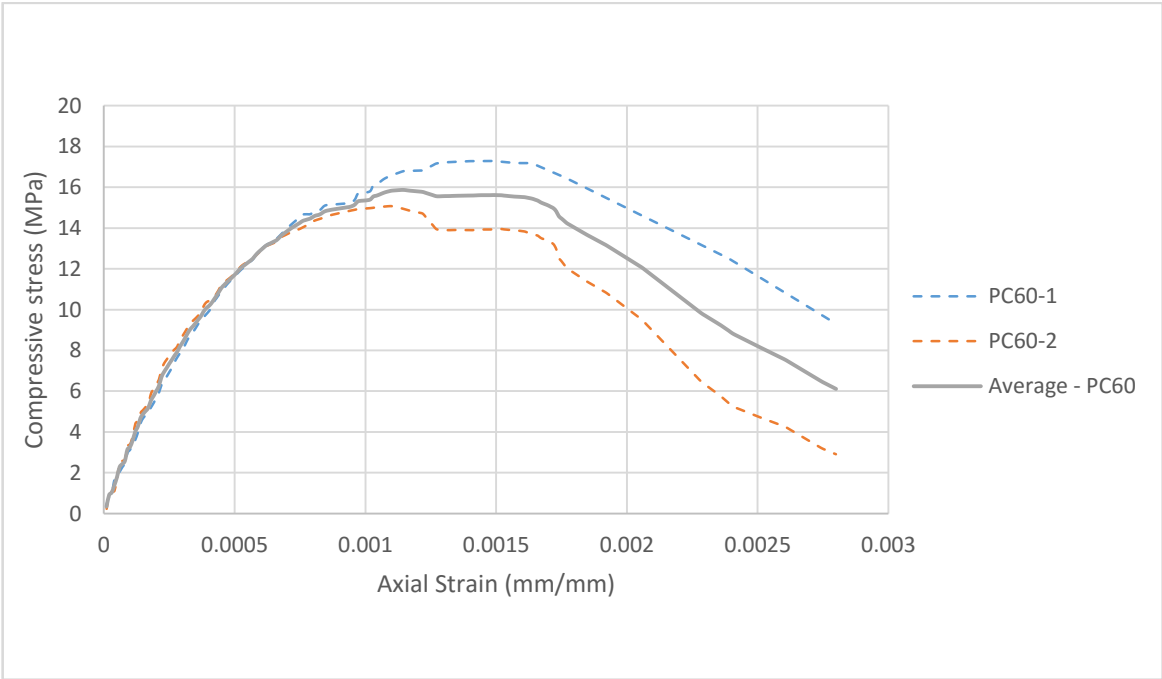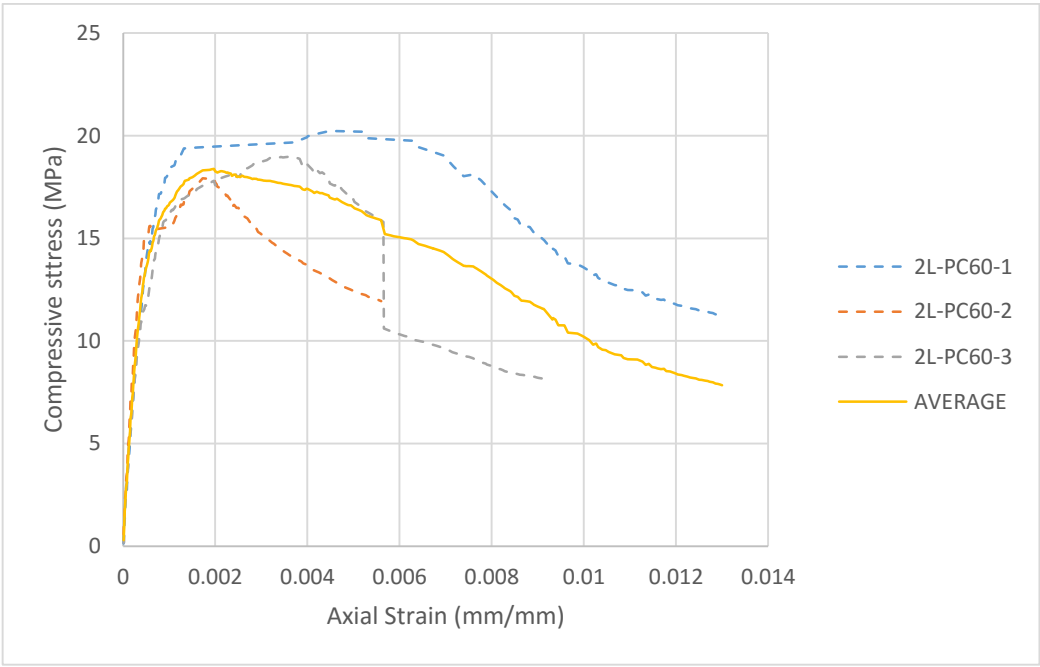
APPENDIX 1

EXPERIMENTAL RESULTS
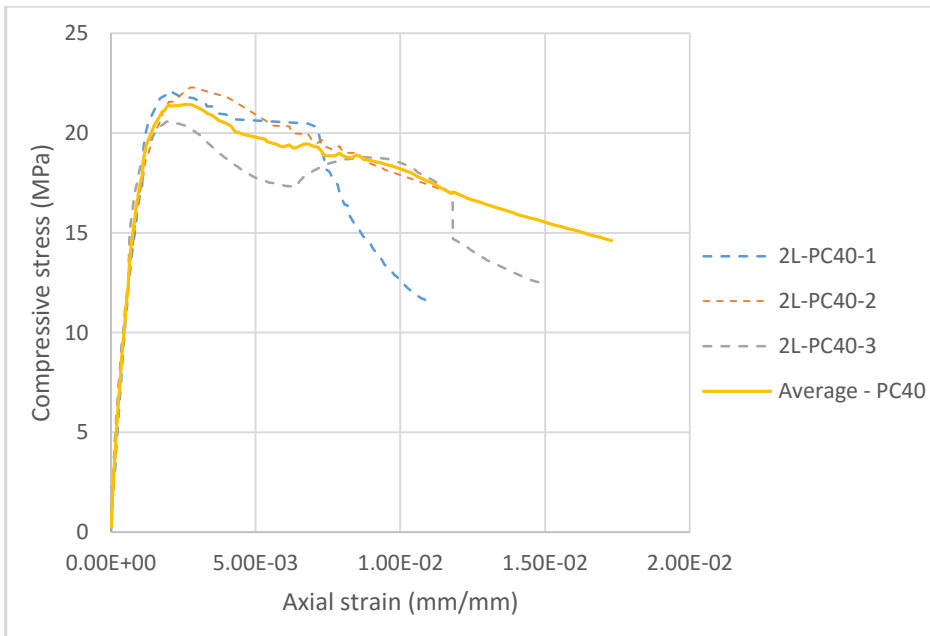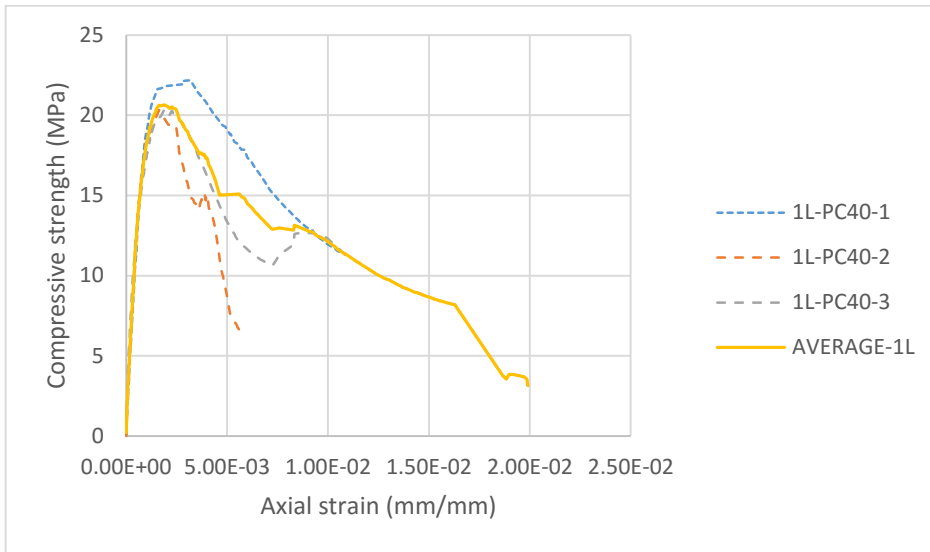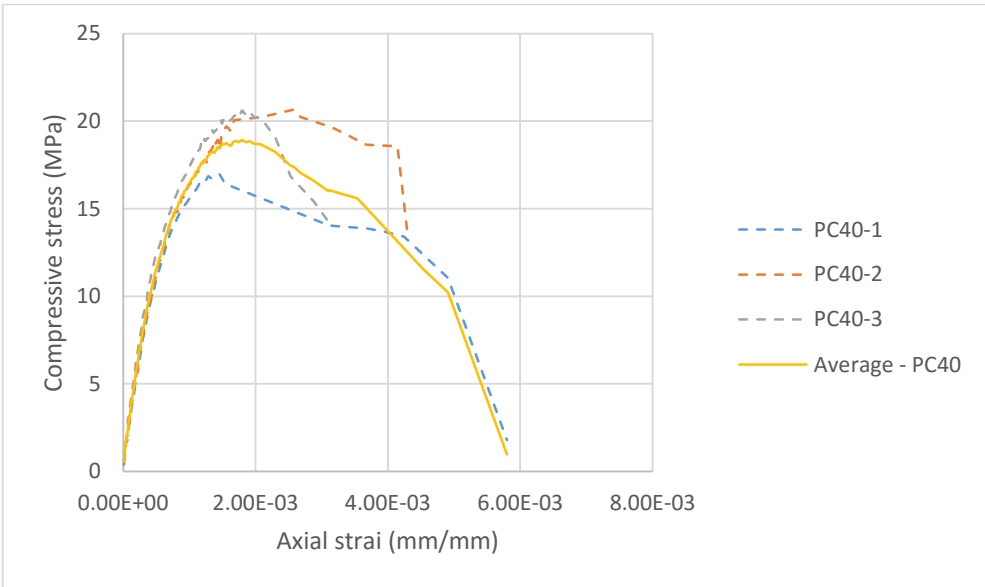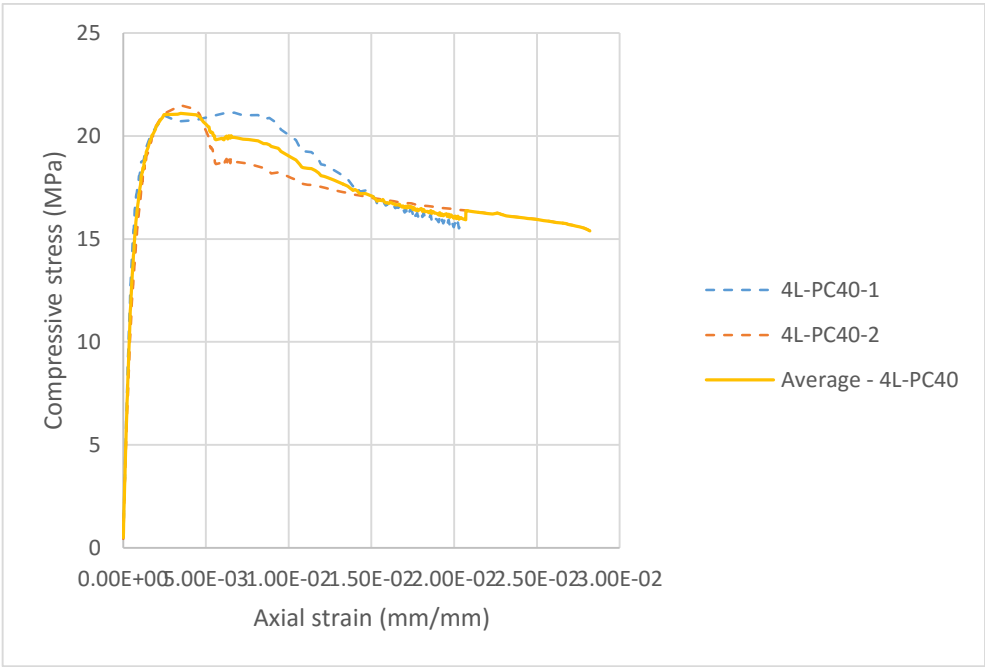
REFERENCES

ACI Committee. (2008). Guide for the design and construction of externally bonded FRP systems for strengthening concrete structures,. *ACI 440.2R-08*. Detroit: American Concrete Institute.

ACI Committee 215. (1975). Considerations for Design of Concrete Structures. *ACI Journal Proceedings*, 71.

Aire, C., Gettu, R., & Cansas, J. (2001). Study of the compressive behavior of concrete confined by fiber reinforced composite. *Composites in Constructions, Proceedings of the Interbnational Conference* (pp. 239-243). Lisse, The Netherlands: A.A. Balkema publishers.

ASTM. (2010). Standard test methods for compressive strength of cylindrical concrete specimens. *ASTM C39*.

ASTM. (2014). Standard for Tensile Properties of Single Fibers. *ASTM D3822-14*.

Awwad, E., Mabsout, M., Hamad, B., Farran, M., & Khatib, H. (2012). Studies on fiber-reinforced concrete using industrial hemp fibers. *Constuction and Building Materials*, 710-717.

Benzaid, R., & Mesbah, H. (2014). The confinement of concrete in compression using CFRP composites – effective design equations. *Journal of Civil Engineering and Management*, 632-648.

Deb, A., & Bhattacharyya, S. (2010). Investigation into the effect of bonding on FRP-wrapped cylindrical concrete columns. *J Compos Construct, 14*(6), 706-719.

Demers, M., & Neale, K. (1999). Confinement of reinforced concrete columns with fiber-reinforced composite sheets – an experimental study. *Canadian Journal of Civil Engineering*, 226-241.

El-Hacha, R., & Abdelrahman, K. (2013). Slenderness effect of circular concrete specimens confined with SFRP sheets. *Composites Part B: Engineering*, 153-166.

Elsanadedy, H., Al-salloum, Y., Alsayed, S., & Iqbal, R. (2012). Experimental and numerical investigation of size effects in FRP-wrapped concrete columns. *Construction and Building Materials*, 56-72.

Gheorghiu, C., Labossiere, P., & Proulx, J. (2004). Fatigue and Post-Fatigue Quasi-Static Performance of RC-Beams Externally Strengthened with CFRPs. *FRP Composites in Civil Engineering-CICE 2004* (p. 433). Adelaide, Australia: Proceeding of the 2nd International Conference on FRP Composites in Civil Engineering-CICE 2004.

Harries, K., & Kharel, G. (2002). Behaviour and modeling of concrete subjected to variable confining pressure. *ACI MATER J*, 180-189.

Kahn, M. E., & Levinson, D. M. (2011). *Fix it First, Expand it Second, Reward.* Washington, DC: Hamilton Project publisher.

Khan, M. R. (2011). Fineness and tensile properties of hemp (Cannabis sativa L.) fibres. *Biosystems Engineering*, 9-17.

Kono, S., Inazumi, M., & Kaku, T. (n.d.). Evaluation of confing effects of CFRP sheets on reinforced concrete members. In: Proceeding of 2nd International conference on Composites in Infrastructure. *Tucson,* , (pp. 343-355). Arizon.

Lam, L., & Teng, J. (2001). A new stress-strain model for FRP-confined concrete. In: Teng JG, editor. Proceeding on international conference on FRP composites in civil engineering., (pp. 283-292).

Lam, T., & Teng, J. (2003). Design-oriented stress–strain model for FRP-confined concrete. *Construction and Building Materials, 17*(6-7), 471-489.

Mander, J. B., Priestley, M. J., & Park, R. (1988). THEORETICAL STRESS-STRAIN MODEL FOR CONFINED CONCRETE. *Journal of Structural Engineering*, 1804-1826.

Mirmiran, A., Shahawy, A., Samaan, M., EI Echary, H., Mastrapa, J., & Pico, O. (1998). Effect of column parameters on FRP-confined concrete. *JOURNAL OF COMPOSITES FOR CONSTRUCTION, 2*(4), 165-185.

Pan, J., Xu, T., & Hu, Z. (2007). Experimental investigation of load carrying capacity of the slender reinforced concrete columns wrapped with FRP. *Construction and Building Materials*, 1991-1996.

Placet, V. (2009). Characterization of the thermo-mechanical behaviour of Hemp fibres intended for the manufacturing of high performance composites. *Composites Part A: Applied Science and Manufacturing*, 1111-1118.

Raithby, K. (1980). External Strengthening o f Concrete Bridges with Bonded Steel
PlatesTransport and Road. Volume 612 of Supplementary report, Wokingham,
Berks, UK: Transport and Road.

Sadeghian, P., Shekari, A., & Mousavi, F. (2009). Stress and Strain Behavior of Slender
Concrete Columns Retrofitted with CFRP Composites. *Journal of REINFORCED
PLASTICS AND COMPOSITES*, 2387-2396.

Sawpan, M. A. (2011). Effect of various chemical treatments on the fibre structure and
tensile properties of industrial hemp fibres. *Composites Part A: Applied Science and
Manufacturing*, 888-895.

Sen, T., & Reddy, H. (2014). Efficacy of bio derived jute FRP composite based technique
for shear strength retrofitting of reinforced concrete beams and its comparative
analysis with carbon and glass FRP shear retrofitting schemes. *Sustainable Cities
and Society*, 105-124.

Sena, T., & Reddy, H. (2014). Flexural strengthening of RC beams using natural sisal and
artificial carbon and glass fabric reinforced composite system. *Sustainable Cities
and Society*, 195-206.

Shahzad, A. (2011). Hemp fiber and its composites – a review. *Journal of Composite
Materials*, 973-986.

Silva, M., & Rodrigues, C. (2006). Size and Relative Stiffness Effects on Compressive
Failure of Concrete Columns Wrapped with Glass FRP. *Journal of Materials in
Civil Engineering*, 334-342.

Spoelstra, M., & Monti, G. (1999). FRP-confined concrete model. *J Compos Constr, 3*(3),
143-150.

Wu, Y., & Zhou, Y. (2010). Unified strength model based on Hoek-Brown failure criterion
for circular and square concrete columns confined by FRP. *J Compos Constr*, 175-
184.

Xiao, Y., & Wu, H. (2003). Compressive behavior of concrete confined bu various type of
FRP composite jackets. *Journal of Reinforced Plastics and Composites, 22(13)*,
1187-1201.

Yan, L., & Chouw, N. (2012). Behaviour and analytical modelling of flax fibre reinforced
polymer tube confined plain concrete and coire fibre reinforced concrete. *J Compos
Mater*, DOI: 10.1177/0021998312454691.

Yan, L., & Chouw, N. (2013). Compressive and flexural behavior and theoretical analysis of flax fiber reinforced polymer tube encased coir fiber reinforced concrete composite. *Materials and Design*, 801-811.

Yan, L., & Chouw, N. (2013). Experimental study of flax FRP tube encased coir fibre reinforced concrete composite column. *Construction and Building Materials* , 1118-1127.

Yan, L., Duchez, A., & Chouw, N. (2013). Effect of bond on compressive behavior of flax fiber reinforced polymer tube-confined coir fiber reinforced concrete. *Journal of REINFORCED PLASTICS & COMPOSITES, 32*(4), 273-285.

Youssef, M., Feng, Q., & Mosallam, A. (2007). Stress-strain models for concrete confined by FRP composites. . *Composites Part B*, 614-628.